

UNIVERSITI
TEKNOLOGI
PETRONAS

Final Report

Final Year Project 2

Development of 3D Crane PID Controller System via State-space Approach

by

Nur Zuhdi bin Zailan

10941

Supervisor

Dr. Nordin bin Saad

Bachelor of Engineering (Hons)
(Electrical and Electronics Engineering)

September 2011

Universiti Teknologi PETRONAS
Bandar Seri Iskandar
31750 Tronoh
Perak Darul Ridzuan

CERTIFICATION OF APPROVAL

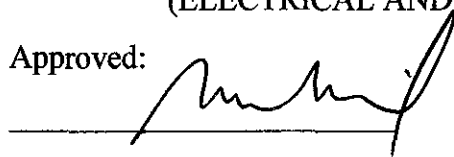
Development of 3D Crane PID Controller System via State-space Approach

By

Nur Zuhdi bin Zailan

A project dissertation submitted to
Electrical and Electronics Engineering Programme
Universiti Teknologi PETRONAS
in partial fulfillment of the requirements for the
BACHELOR OF ENGINEERING (Hons)
(ELECTRICAL AND ELECTRONICS ENGINEERING)

Approved:



Dr. Nordin Bin Saad

Project Supervisor

UNIVERSITI TEKNOLOGI PETRONAS

Dr. Nordin Saad

Lecturer

Electrical & Electronics Engineering Programme

Universiti Teknologi PETRONAS

31750 Tronoh,

Perak Darul Ridzuan, MALAYSIA

TRONOH, PERAK

SEPTEMBER 2011

CERTIFICATION OF ORIGINALITY

This is to certify that I am responsible for the work submitted in this project, that the original work is my own except as specified in the references and acknowledgements, and that the original work contained herein have not been undertaken or done by unspecified sources or persons.



JR ZUHDI BIN ZAILAN

ABSTRACT

This progress report is basically present the research that has been done so far based on the chosen topic, which is **Development of 3D Crane PID Controller System via State-space Approach**. The objective of the project is to be able to determine the 3D Crane and 2D Crane dynamics using the state-space approach and applies the Proportional-Integral-Derivative controller algorithm into the system for improvement. This dynamic equation is important for simulating the 2D crane in computer using Matlab and Simulink software and designing a suitable controller for the 2D crane. The mathematical equation for 2D crane can be modeled dynamically using various approaches such as Lagrange-Euler's Method and Newton-Euler's Method. After the success of producing the 2D Crane dynamics, the mathematical formulation of 3D Crane dynamics will take place. Using the appropriate approach, the mathematical or state space equation of the 3D Crane dynamics will be produced for simulation in Matlab and Simulink Software. Finally, the Proportional-Integral-Derivative controller will be added into the system for increasing of crane reliability and productivity.

TABLE OF CONTENTS

ABSTRACT.									i
CHAPTER 1:		INTRODUCTION
1	1.0	Project Background	1
	1.1	Problem Statement	2
	1.2	Project Objectives	2
	1.3	Scope of Study	3
	1.4	Methodology	3
	1.4	FYP Flow Chart.	4
CHAPTER 2:		LITERATURE REVIEW
5	2.0	Introduction to 3D Crane	5
	2.1	3D Crane System	8
	2.2	PID Controller.	9
	2.3	PID Control Systems of 3D Crane	10
	2.4	Dynamic Modeling of Cranes.	11
CHAPTER 3:		METHODOLOGY
12	3.0	Introduction to 2D Crane Mathematical Formulation							12
	3.1	2D Crane Modeling	13
	3.0	Introduction to 3D Crane Mathematical Formulation							14
	3.3	Development of 3D Crane System.	14
	3.4	3D Crane Modeling	16
	3.5	Tools Required	16

CHAPTER 4:

18

	RESULT AND ANALYSIS	
4.0	2D Crane Model Discription	17
4.1	Dynamic Equation Derivation. . . .	17
4.2	Linearization of the 2D Crane System. . . .	20
4.3	General State-space Representation of the System	20
4.4	Transfer Function of 2D Crane System	21
4.5	Dynamic Behavior Simulation of 2D Crane	23
4.6	Sway Motion of 2D Crane	24
4.7	Trolley Position	26
4.8	Sway Angle	26
4.9	System Analysis and Discussion	27
4.9.1	Input Force	27
4.9.2	Length of the Hoisting Rope	29
4.9.3	Payload Mass	32
4.10	Simulation of 2D Crane Using Transfer Function	34
4.11	Formulation of 2D Crane Using State-space Approach	36
4.11.1	Control Canonical Form of 2D Crane.	37
4.11.2	Observer Canonical Form of 2D Crane	39
4.12	Simulation of 2D Crane Using State-space Approach	41
4.13	Simulation of PID Controller of 2D Crane System	43
4.13.1	Time Delay	46
4.13.2	Frictional Force Disturbance	47
4.13.3	Harmonic Force Disturbance	48
4.14	Simulation of PID Controller with Derivative Filter of 2D Crane System	50

CHAPTER 5:		DISCUSSION
47	5.0	Project Reliability	61
	5.1	Future Development and Application.	61
CHAPTER 6:		CONCLUSION
48	6.0	Conclusion	63
REFERENCES	64
APPENDIX	65

LIST OF FIGURE

- Figure 1:** Flow Chart for Modeling and Control of 3D Crane
- Figure 2:** 3D Crane Model
- Figure 3:** 3D Crane
- Figure 4:** 2D Crane Dynamics
- Figure 5:** 3D Crane Dynamics
- Figure 6.1:** 2D Crane System
- Figure 6.2:** PID Controller for 2D Crane System
- Figure 7:** DEE for 2D Crane System
- Figure 8:** Bang-bang Input Force, 1N
- Figure 9:** Trolley Position (m)
- Figure 10:** Sway Angle (rad)
- Figure 11:** Bang-bang Input Force at 1N, 2N and 4N
- Figure 12:** Trolley Position for Force at 1N, 2N and 4N
- Figure 13:** Sway Angle for Force at 1N, 2N and 4N
- Figure 14:** Trolley Position for Hoisting Rope length, l of 0.305m, 0.2m and 0.5m
- Figure 15:** Sway Angle for Hoisting Rope length, l of 0.305m, 0.2m and 0.5m
- Figure 16:** Trolley Position for Trolley Mass, M of 0.5 kg, 1 kg and 2 kg
- Figure 17:** Sway Angle for Trolley Mass, M of 0.5 kg, 1 kg and 2 kg
- Figure 18:** Trolley Position for Payload Mass, M of 0.4 kg, 0.8 kg and 1.6 kg
- Figure 19:** Sway Angle for Payload Mass, M of 0.4 kg, 0.8 kg and 1.6 kg
- Figure 20:** Block Diagram of 2D Crane System
- Figure 21:** Trolley Position (m)
- Figure 22:** Sway Angle (rad)
- Figure 23:** Signal Flow Graph Block Diagram for 2D Crane
- Figure 24:** Signal Flow Graph of Observer Canonical Form
- Figure 25:** Signal Flow Graph Block Diagram for 2D Crane

- Figure 26:** Trolley Position (m)
- Figure 27:** Sway Angle (rad)
- Figure 28:** PID Controller of 2D Crane
- Figure 29:** PID Controller of 2D Crane System using State-space Approach
- Figure 30:** Trolley Position output for PID Controller of 2D Crane System
- Figure 31:** Sway Angle output for PID Controller of 2D Crane System
- Figure 32:** Trolley Position output for PID Controller of 2D Crane System with Delay
- Figure 33:** Sway Angle output for PID Controller of 2D Crane System with Delay
- Figure 34:** Trolley Position output for PID Controller of 2D Crane System with Frictional Force Disturbance and Delay
- Figure 35:** Sway Angle output for PID Controller of 2D Crane System with Frictional Force Disturbance and Delay
- Figure 36:** Harmonic Force into the 2D Crane System; $y(t) = 1 \sin 5t$
- Figure 37:** Trolley Position output for PID Controller of 2D Crane System with Harmonic Force Disturbance and Delay
- Figure 38:** Sway Angle output for PID Controller of 2D Crane System with Harmonic Force Disturbance and Delay
- Figure 39:** PID Controller with Derivative Filter of 2D Crane
- Figure 40:** Trolley Position Output for PID Controller with Derivative Filter of 2D Crane System
- Figure 41:** Sway Angle Output for PID Controller with Derivative Filter of 2D Crane System

LIST OF TABLE

Table 1: Basic Parts of 3D crane

CHAPTER 1

INTRODUCTION

1.0 Project Background

3D cranes are an important industrial structure that are often used in building construction, factories and oil rig/platform or even on the navy shipyard. Besides that, they are also widely constructed to transport heavy loads and hazardous material in shipyards, factories, nuclear installation, and high building construction. These cranes are usually operated manually by crane operators. Generally, operators use the joystick and also the acceleration pedal to control the movement and direction of the cranes. On the shipyard, they are mounted to transfer cargo between ships or on the harbor pavements to transfer cargo between ships and offshore.

Basically, the movement of cranes has no prescribed path. They are used to move load from one point to another. With the size of these cranes becoming larger and the motion expected to be faster, the process of controlling them become difficult. As 3D cranes have to run under different operating conditions, which make closed-loop control preferable.

The requirement of precise sway control of 3D cranes implies that the residual sway of the payload should be zero or near to zero. Over the years, investigations have been carried out to devise efficient approaches to reduce the payload sway of 3D cranes. As the performance requirements imposed by the industry become more severe, the need to understand how to model and control 3D cranes become an

1.3. Scope of Study

For this project, scopes of study are limited to certain area:

a) **Operator-in-the-loop approach**

Operator-in-the-loop approach means that the input of the model will be the accelerations of the links of the 3D crane resulting from the control of an operator using acceleration pedals and joystick.

b) **Proportional Integral Derivative, PID Controller technique**

The application of Proportional-Integral-Derivative, PID Controller will be applied on the 3D crane System to optimize the application and increase the reliability of the 3D crane.

1.4. Methodology

For this project, the approaches being used to carry out the project are:

a) **Literature review**

Many technical papers and online materials regarding to the modeling technique of 3D crane are referred. Besides, article about the PID Controller applied on 3D crane of various schemes have been read and analyzed.

b) **Matlab software**

Matlab software is used to calculate complex mathematical solutions and to model the 3D crane mathematically. The PID Control schemes are designed and simulate using Matlab Simulink toolbox.

1.5. FYP Flow Chart

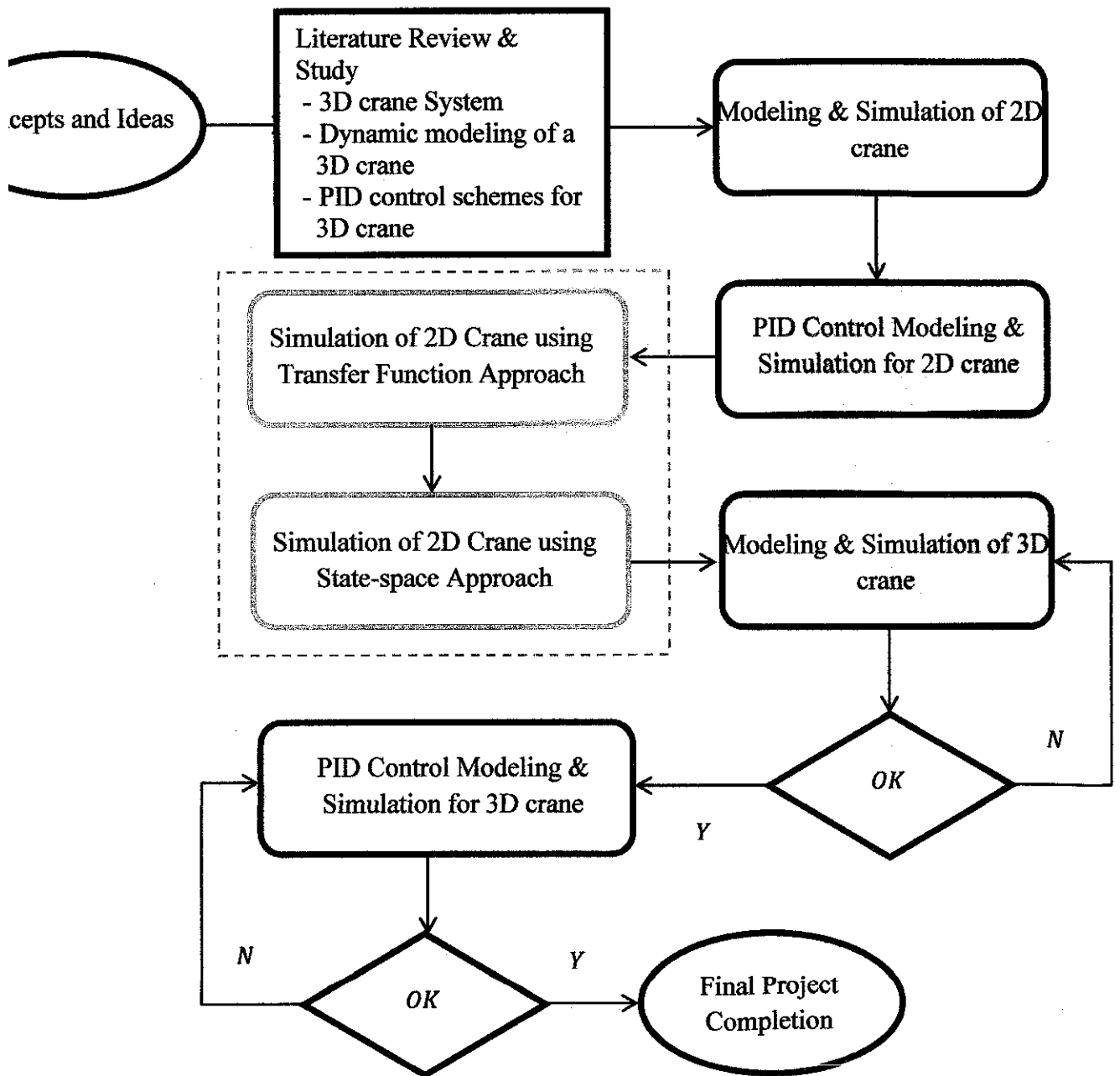


Figure 1: Flow Chart for Modeling and Control of 3D Crane

CHAPTER 2

LITERATURE REVIEW

This chapter consists of some information about crane system and also an overview of the literature that has been published in relation to crane control.

2.0 Introduction to 3D Crane

A crane is a mechanical machine that equipped with a wire rope drum, wire rope or chain and shaves that can be used both to lift and lower materials and to move them horizontally. It uses a combination of one or more simple machines to create mechanical advantages and thus move load beyond the normal capability of a human. This is important to make sure the crane is able to lift a heavy load within required time frame from one location to the other. Crane is commonly employed in the transport industry for the loading and unloading of freight, in the construction industry for the movement of materials and in the manufacturing industry for assembling of heavy equipment in a higher floor which wasn't able to reach by human capability.

In history of crane, the first constructed cranes were invented by ancient Greeks where the earliest crane was build from wood, but cast iron and steel took over with the coming of the Industrial Revolution. Before the mechanical power which is steam engines and hydraulic system equipped crane, the first invented crane were powered by men or beasts as burden. Modern crane usually use internal combustion engines or electric motors and hydraulic systems to provide a much greater lifting capability than was previously use. The introduction of the winch and

pulley hoist soon leads to a widespread replacement of ramps as the main means of vertical motion. As the demand of constructing a high power crane increases, the facilities of increasing crane effectiveness required to be proportional.

In designing a crane, there are two major consideration which is first the crane must be able to lift a load of a specific range of weight and second it must remain stable and not to drop or topple over when the load is lifted and moved to another locations. In the direction of lifting and moving, the load must be able to avoid any obstacle in the way as to avoid damage to surrounding. The cranes also just like any other machine, where it obeys the principle of conservation of energy. Meaning that the energy delivered to the load must not exceed the energy put into the machine. As example, if a pulley system multiplies the applied force by ten, then the load moves only one tenth as far as the applied force. And since energy equal to force times distance, the output energy is keep roughly equal to the input energy. But sometimes the output energy is slightly less than the input energy due to the lost cause by friction in the rail and inefficiency of the mechanical machine involved.

For stability of a crane, the sum of all moments about any point such as the base of the crane must equal to zero. In real life, the magnitude of load that is permitted to be lifted or known as “rated load” must be less than the load that will cause the crane to tip. The rated load is usually in a manner of lowest and highest that can be supported by the mechanical components involved in the system as it is important to avoid any mechanical structure to degrade faster and reduce the efficiency of the overall system.

Movement of 3D crane consists of a three dimensional direction which is x, y and z direction respectively. The difference between 3D crane compare to any other crane such as Spider Crane is that 3D crane has better structure and higher Safety Integrity Level, SIL for its instrument and mechanical structure since the failure of 3D crane is easily repaired and spotted in the first place before accident occur. In increasing demand of using 3D crane to transfer heavy and big stuff from one place to the other, a reliable controller is required to control the crane to work at higher accuracy and reliability.

X-Drive	<ul style="list-style-type: none"> • Important part that help to move the load and crane in the x-direction • Consists of a Motor that can support the load and drive the crane to the x-direction as required
Y-Drive	<ul style="list-style-type: none"> • Useful part that help to move the load and crane in the y-direction • Consists of a Motor that can support the load and drive the crane to the y-direction as required
Z-Drive	<ul style="list-style-type: none"> • Parts that help to lift the load and crane in the z-direction • Consists of a Motor that can support the load and avoid obstacles while following the x and y direction route
X-Position Sensor	<ul style="list-style-type: none"> • Part that help to measure the x position of a main hook
Y-Position Sensor	<ul style="list-style-type: none"> • Part that help to measure the y position of a main hook
Z-Position Sensor	<ul style="list-style-type: none"> • Part that help to measure the length of the rope
Angle Sensor	<ul style="list-style-type: none"> • Part that help to measure the length of angle in x and y direction

Table 1: Basic Parts of 3D crane

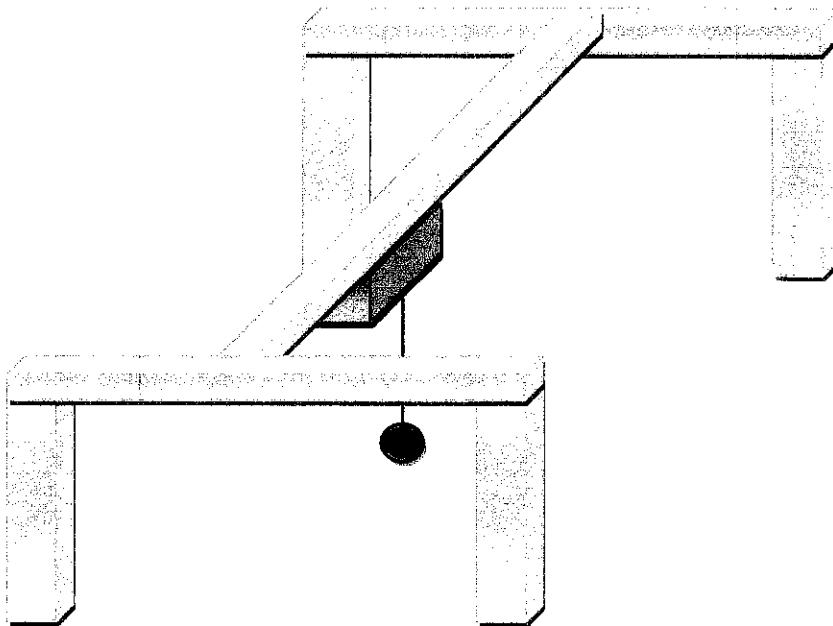


Figure 2: 3D Crane Model

2.1 3D Crane System

Recently designed 3D cranes are larger and have higher lifting capacities and travel speeds. To achieve high productivity and to comply with the safety requirements, these cranes require effective controllers such as anti sway controls. Most of the anti sway control of the 3D crane is performed manually by skillful human operators who combine their intuition, experience and skill to manipulate a load hanging on a hoisting cable by stopping the trolley near the desired position and then letting the payload to stop oscillating gradually by a further gentle movement of the trolley. However, this poses some practical problems, particularly due to human fatigue that in turn may affect significantly the performance and operation of the 3D crane.

In addition, 3D cranes are mostly equipped with cabled hoisting mechanism, which are prone to the load sway problems due to the fact that the assembly of the cable-hook-payload results in complex system dynamics. Even in the absence of external disturbances, inertia forces due to the motion of the crane can induce significant payload oscillations. This problem is exacerbated by the fact that 3D cranes are usually lightly damped, which implies that any transient motion takes a long time to dampen out [1]

For this reason, the payload sway angle should be kept to a minimum; otherwise, a large payload sway angle during transportation may cause damage to the payload, surrounding equipment or even personnel. If the pendulum-like oscillations of the payload can be constrained using an appropriate method, there will be a number of benefits such as having greater yield and safety margin, enabling higher operating speed, enhancing work quality and creating greater throughput for a given installed capacity. Besides, most actual systems are influenced by noise and external disturbances including 3D crane. These disturbances such as wind, unstable mounting and others may degrade the performance of the 3D crane.

Previously, many approaches have been proposed to solve the above stated problem. An approach known as input shaping technique is widely used as an open-loop

control strategy for 3D cranes. The controller using this strategy will accelerate the trolley in steps of constant acceleration. Although there will be effectively no residual oscillations but large transient oscillations will happen during the transportation. Besides, input-shaping techniques are limited by the facts that (i) they are sensitive to variations in the parameter values about the nominal values and changes in the initial conditions and external disturbances and (ii) they require 'highly accurate values of the system parameters' to achieve satisfactory system response [2].

2.2 Proportional-Integral-Derivative, PID Controller

PID is stand for Proportional-Integral-Derivative. This type of controller is widely used in industrial application since 1940s and remains the most often algorithm today. It is because of their simplicity, robustness, and successful practical applications. A PID controller also calculates an "error" value as the difference between a measured process variable and a desired set point. The time-domain controller algorithm for PID controller is given below:

$$MV(t) = K_c \left(E(t) + \frac{1}{T_I} \int_0^t E(t') dt' + T_d \frac{dE(t)}{dt} \right) + I$$

The PID controller calculation (algorithm) involves three separate parameters, and is accordingly sometimes called three-term control: the proportional, the integral and derivative values, denoted P , I , and D . The proportional value determines the reaction to the current error, the integral value determines the reaction based on the sum of recent errors, and the derivative value determines the reaction based on the rate at which the error has been changing. The weighted sum of these three actions is used to adjust the process via a control element such as the position of a control valve or the power supply of a heating element. Heuristically, these values can be interpreted in terms of time: P depends on the present error, I on the accumulation of past errors, and is a prediction of future errors, based on current rate of change[3].

By tuning the three constants in the PID controller algorithm, the controller can provide control action designed for specific process requirements. The response of the controller can be described in terms of the responsiveness of the controller to an error, the degree to which the controller overshoots the set point and the degree of system oscillation. Note that the use of the PID algorithm for control does not guarantee optimal control of the system or system stability.

Some applications may require using only one or two modes to provide the appropriate system control. This is achieved by setting the gain of undesired control outputs to zero. A PID controller will be called a PI, PD, P or I controller in the absence of the respective control actions. PI controllers are fairly common, since derivative action is sensitive to measurement noise, whereas the absence of an integral value may prevent the system from reaching its target value due to the control action.

This controller often provides acceptable control even in the absence of tuning, but performance can generally be improved by careful tuning, and performance may be unacceptable with poor tuning. The example methods for tuning a PID loop are manual tuning, Ziegler-Nichols, Software tools and Cohen-coon.

2.3 PID Control System for 3D Crane

The studies conducted by Sanda Dale, Gianina Gabor, Cornelia Gyrodi and Doina Zmaranda aim to investigate the control performance of an interpolative control algorithm applied on a complex nonlinear system. The study is basically recognized PID Controller as one of the most useful control algorithm that is highly used in industrial and complex mechanical system. PID algorithm is known as one of the most used control law due to its effectiveness, simplicity and large possibility of implementation [4].

The construction of 3D Crane with PID Controller Algorithm was used to eliminate the external disturbance that will lead to the inefficiency of the lifting and

transfer of heavy loads from one location to the other. The PID Controller with define parameters of disturbance can lead to a productive mechanical machine which will increase the plant effectiveness and reliability. The PID Controller need to be defined first based on the structural construct of the 3D Crane in order to avoid instability of the system.

2.4 Dynamic Modeling of Crane

Figure 3 illustrate 3D cranes that are modeled by B. Kiss, J. Levine and P. Mullhaupt. The Dynamic equation of this 3D crane are obtained using Lagrange's multiplier associated to geometric constrains between generalized coordinates. This approach provides a simple way to show differential flatness for all crane of the class and to generate compact numerical simulation software. The main advantage of this approach can be seen in two applications, namely detecting the flatness property and computing the flat output on the one hand and simulating the system without need to express it in explicit form to achieve simpler computation through with a large number of variables on the other hand. In this paper, the flatness property is proven to hold the modeled class of cranes. This property is useful for both motion planning purpose and for closed control.

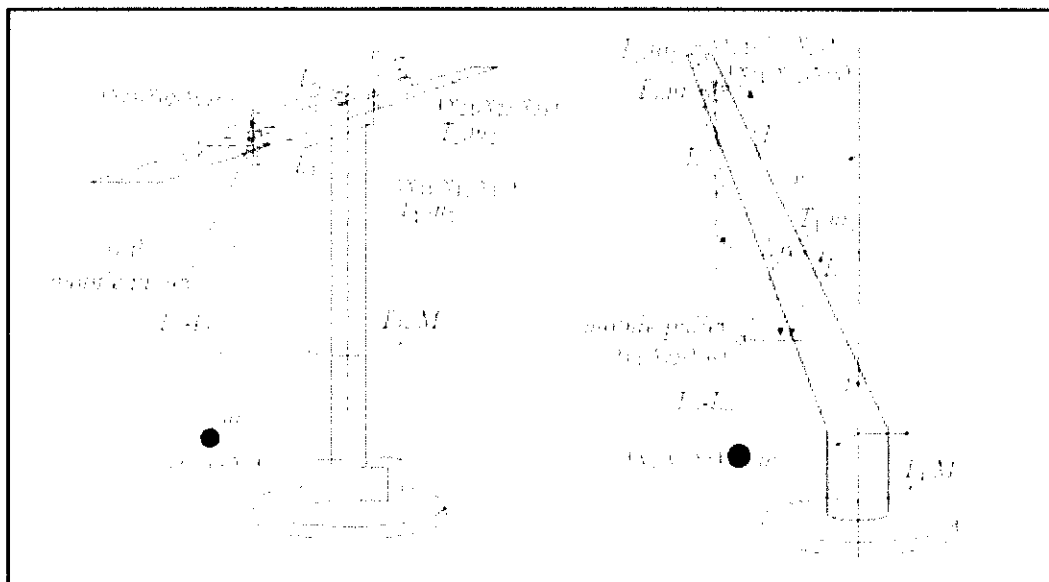


Figure 3: 3D Crane

CHAPTER 3

METHODOLOGY

3.0 Introduction to 2D Crane Mathematical Formulation

2D Crane dynamic equation is concern with mathematical formulation of equations for the crane arm or joint motion where these set of mathematical equation will describe the dynamic behavior of the 2D Crane. This dynamic equation is important for simulating the 3D crane in computer using Matlab and Simulink software and designing a suitable controller for the 3D crane. The mathematical equation for 3D crane can be modeled dynamically using various approaches such as Lagrange-Euler's Method and Newton-Euler's Method. For this project, Lagrange-Euler's Method is used because Lagrange-Euler's methods are more simple and systematic and it will give a set of dynamic equation in a compact matrix form which is appealing from the control view point.

The dynamic model for the 2D crane is derived by using Lagrange-Euler's Method. Based on the figure 4, the equation describing the dynamics of the 2D crane will be determined to obtain the state-space equation of the system. Using Lagrange-Euler's Method, the linear and non-linear equation of the 2D crane will be obtain considering the distance of the rail with the cart denote by x , the distance of the cart denote by y , and angle of oscillation x -axis movement.

3.1. 2D Crane Modeling

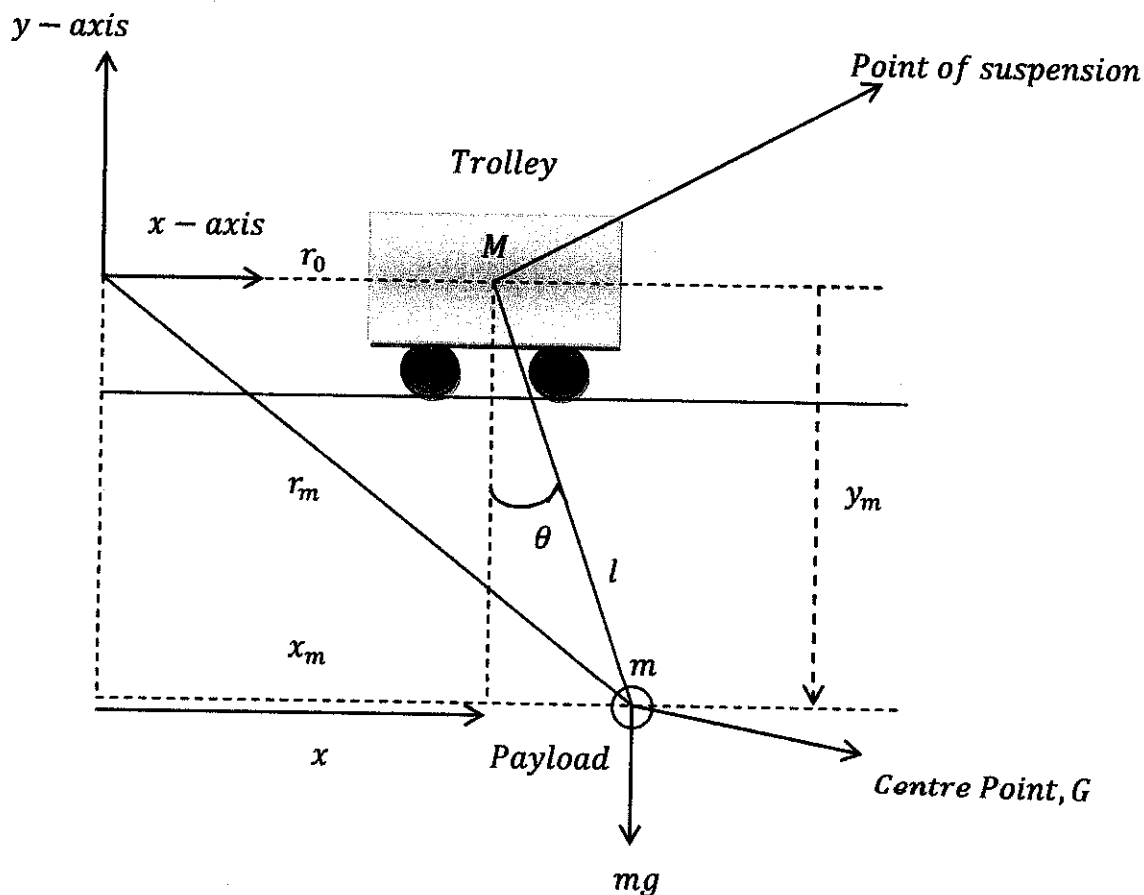


Figure 4: 2D Crane Dynamics

- x = Horizontal position of the trolley (m)
- l = Length of the hoisting rope
- θ = Swing angle of the rope
- M = Mass of the trolley (kg)
- m = Mass of the payload (kg)

The dynamic model for this 2D crane is derived by using Lagrange-Euler's Method. Based on the figure 4, the equation describing the dynamics of the 2D crane will be determined to obtain the state-space equation of the system. Using Lagrange-Euler's Method, the linear and non-linear equation of the 2D crane will be obtain considering the distance of the rail with the cart denote by x , the distance of the cart denote by y , and angle of oscillation x -axis movement.

3.3 Introduction to 3D Crane Mathematical Formulation

3D crane dynamic equation is concern with mathematical formulation of equations for the 3D crane arm or joint motion where these set of mathematical equation will describe the dynamic behavior of the 3D crane. This dynamic equation is important for simulating the 3D crane in computer using Matlab and Simulink software and designing a suitable controller for the 3D crane. The mathematical equation for 3D crane can be modeled dynamically using various approaches such as Lagrange-Euler's Method and Newton-Euler's Method. For this project, Lagrange-Euler's Method is used because Lagrange-Euler's methods are more simple and systematic and it will give a set of dynamic equation in a compact matrix form which is appealing from the control view point.

3.4 Development of 3D Crane System

The 3D crane developed in this project has the ability to move in the x, y and z direction which is in three dimensional direction. The payload can be lifted and lowered in the z-direction. Both the rail and cart are capable of horizontal motion in the x-direction. The cart is capable of horizontal movement along the rail in the y-direction. Therefore, the payload attached to the end of the lift line can move freely in 3-dimensions. The 3D crane is driven by three DC Motor. There are five identical measuring encoders measuring five state variables, the cart coordinate in the horizontal plane, the lift-line length, and two deviation angles of the payload.

Angles are measured in the manner of x and y-direction movement which is namely α and β . The sway angle produce in the z-direction is assumed to be small and approaching zero.

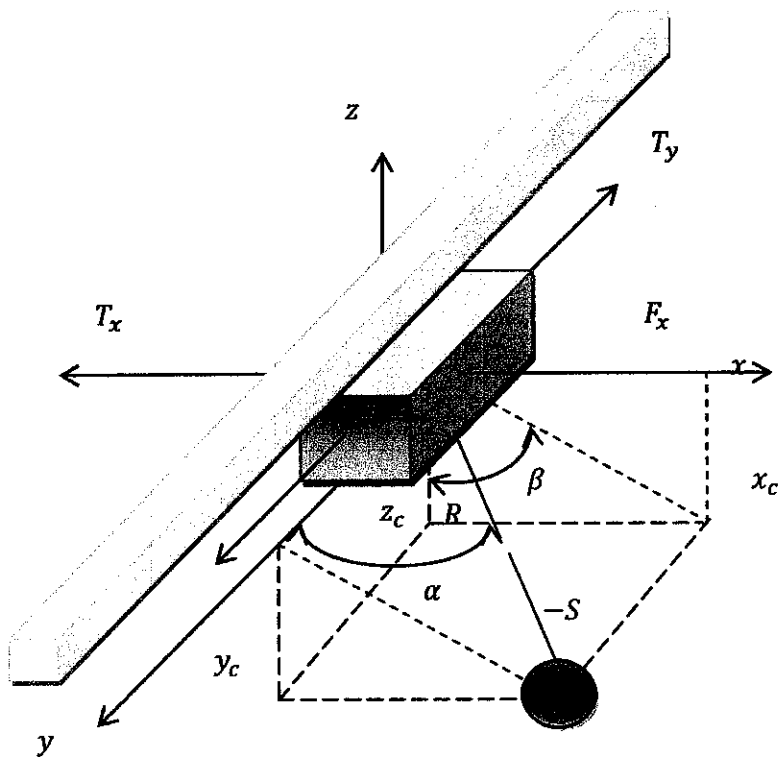


Figure 5: 3D Crane

There are 5 measured quantities:

- x_w denotes the distance of the rail with the cart
- y_w denotes the distance of the cart
- R denotes the length of the lift line
- α denotes the angle between y -axis and the lift line
- β denotes the angle between the negative direction on the z -axis and the projection of the lift line onto the xz -plane

m_c	-	Mass of the payload
m_w	-	Mass of the cart
m_s	-	Mass of the moving rail
x_c, y_c, z_c	-	Coordinates of the payload
S	-	Reaction force in the lift-line acting on the cart
F_x	-	Force driving the rail with cart
F_y	-	Force driving the cart along the rail
F_R	-	Force controlling the length of the lift-line
T_x, T_y, T_R	-	Friction forces

3.5. 3D Crane Modeling

The dynamic model for this 3D crane is derived by using Lagrange-Euler's Method. Based on the figure 4, the equation describing the dynamics of the 3D crane will be determined to obtain the state-space equation of the system. Using Lagrange-Euler's Method, the linear and non-linear equation of the 3D crane will be obtain considering the distance of the rail with the cart denote by x , the distance of the cart denote by y , length of the line denote by R , angle of oscillation respected to y and x -axis movement.

By using the state-space approach the dynamics of the 3D crane will be simulated in Matlab to optimize the equation and for simulation of the proposed system. Using the Matlab/Simulink, the 3D crane dynamics will be constructed and simulated accordingly to produce the functional 3D crane. After that, the construction for the Proportional-Integral-Derivative, PID Controller will take place to be applied into the system to increase the reliability in term of speed and sway angle. The tuning constants for the PID Controller will be determine as these tuning constants is tuned accordingly based on the three tuning goals which are controlled variable behavior, model error and manipulated variable behavior. [5]

3.6. Tools Required

The tools required for this project is Matlab/Simulink Software which is important to be used in simulating the dynamics of the 2D Crane and 3D Crane designed. Most of the time, this project will be using Matlab and Simulink Software to produce the graph and other related information of the 2D Crane and 3D Crane system.

CHAPTER 4

SYSTEM MODELING

4.0 2D Crane Model Description

x	=	Horizontal position of the trolley (m)
l	=	Length of the hoisting rope
θ	=	Swing angle of the rope
M	=	Mass of the trolley (kg)
m	=	Mass of the payload (kg)

4.1 Dynamic Equation Derivation

Lagrangian approach is used to derive the equation of motion. Based on figure, the load and trolley position vectors are given by:

$$\bar{r}_m = \{x + l \sin \theta, -l \cos \theta\}$$

$$\bar{r}_0 = \{x, 0\}$$

The **kinetic and potential** energy of the whole system are given by:

$$T = T_{trolley} + T_{payload}$$

$$= \frac{1}{2} M \dot{x}_0^2 + \frac{1}{2} m \dot{r}_m^2$$

$$= \frac{1}{2} M \dot{x}^2 + \frac{1}{2} m (\dot{x}^2 + \dot{l}^2 + l^2 \dot{\theta}^2 + 2\dot{x}\dot{l} \sin \theta + 2\dot{x}l\dot{\theta} \cos \theta)$$

$$\begin{aligned}
P &= mgy_m \\
&= -mgl \cos \theta
\end{aligned}$$

Using the Lagrangian approach, the following equation is derived as:

$$\begin{aligned}
L &= T - P \\
&= \frac{1}{2}M\dot{x}^2 + \frac{1}{2}m(\dot{x}^2 + \dot{l}^2 + l^2\dot{\theta}^2 + 2\dot{x}\dot{l} \sin \theta + 2\dot{x}l\dot{\theta} \cos \theta) + mgl \cos \theta
\end{aligned}$$

Let the generalized forces corresponding to the generalized displacements $\bar{q} = \{x, \theta\}$ be $\bar{F} = \{F_x, 0\}$. Constructing the Lagrangian $L = T - P$ and using Lagrangian's equations:

$$\frac{d}{dt} \left(\frac{\partial L}{\partial \dot{q}_j} \right) - \frac{\partial L}{\partial q_j} = F_j \quad j = 1, 2$$

We will obtain the equation of motion for the gantry crane system. Firstly, the equation of motion associate with the generalized coordinate $q = x$ can be derived as below:

$$\frac{d}{dt} \left(\frac{\partial L}{\partial \dot{x}} \right) - \frac{\partial L}{\partial x} = F_x$$

$$\frac{\partial L}{\partial x} = 0$$

$$\frac{\partial L}{\partial \dot{x}} = M\dot{x} + \frac{1}{2}m(2\dot{x} + 2\dot{l} \sin \theta + 2l\dot{\theta} \cos \theta)$$

$$= M\dot{x} + m\dot{x} + m\dot{l} \sin \theta + ml\dot{\theta} \cos \theta$$

$$\begin{aligned}
\frac{d}{dt} \left(\frac{\partial L}{\partial \dot{x}} \right) &= M\ddot{x} + m\ddot{x} + m(\dot{l} \sin \theta + l\dot{\theta} \cos \theta) + m[l\dot{\theta} \cos \theta + l\ddot{\theta} \cos \theta \\
&\quad + l\dot{\theta}(-\sin \theta) \dot{\theta}]
\end{aligned}$$

$$= (M + m)\ddot{x} + m(\dot{l} \sin \theta + l\dot{\theta} \cos \theta) + m[l\dot{\theta} \cos \theta + l\ddot{\theta} \cos \theta - l\dot{\theta}^2 \sin \theta]$$

$$= (M + m)\ddot{x} + ml(\ddot{\theta} \cos \theta - \dot{\theta}^2 \sin \theta) + 2ml\dot{\theta} \cos \theta + m\dot{l} \sin \theta$$

Thus,

$$\frac{d}{dt} \left(\frac{\partial L}{\partial \dot{x}} \right) - 0 = F_x$$

$$F_x = (M + m)\ddot{x} + ml(\ddot{\theta} \cos \theta - \dot{\theta}^2 \sin \theta) + 2ml\dot{\theta} \cos \theta$$

Secondly, the equation of motion associate with the generalized coordinate $q = \theta$ is as below:

$$\frac{d}{dt} \left(\frac{\partial L}{\partial \dot{\theta}} \right) - \frac{\partial L}{\partial \theta} = 0$$

$$\begin{aligned} \frac{\partial L}{\partial \theta} &= \frac{1}{2} m [2\dot{x}l \cos \theta + 2\dot{x}l\dot{\theta}(-\sin \theta)] + mgl(-\sin \theta) \\ &= \frac{1}{2} m (2\dot{x}l \cos \theta - 2\dot{x}l\dot{\theta} \sin \theta) - mgl \sin \theta \end{aligned}$$

$$\frac{\partial L}{\partial \dot{\theta}} = \frac{1}{2} m (2l^2\dot{\theta} + 2\dot{x}l \cos \theta) - mgl \sin \theta$$

$$\begin{aligned} \frac{d}{dt} \left(\frac{\partial L}{\partial \dot{\theta}} \right) &= \frac{1}{2} m [2l^2\ddot{\theta} + 2l\dot{\theta}(2l) + 2\ddot{x}l \cos \theta + 2\dot{x}l \cos \theta \\ &= \frac{1}{2} m (2l^2\ddot{\theta} + 4l\dot{\theta} + 2\ddot{x}l \cos \theta + 2\dot{x}l \cos \theta - 2\dot{x}l\dot{\theta} \sin \theta) \end{aligned}$$

$$\frac{d}{dt} \left(\frac{\partial L}{\partial \dot{\theta}} \right) - \frac{\partial L}{\partial \theta} = 0$$

$$\begin{aligned} &= \frac{1}{2} m (2l^2\ddot{\theta} + 4l\dot{\theta} + 2\ddot{x}l \cos \theta + 2\dot{x}l \cos \theta - 2\dot{x}l\dot{\theta} \sin \theta) \\ &\quad - \frac{1}{2} m (2\dot{x}l \cos \theta - 2\dot{x}l\dot{\theta} \sin \theta) + mgl \sin \theta \\ &= 2l^2\ddot{\theta} + 4l\dot{\theta} + 2\ddot{x}l \cos \theta + 2\dot{x}l \cos \theta - 2\dot{x}l\dot{\theta} \sin \theta - 2\dot{x}l \cos \theta \\ &\quad + 2\dot{x}l\dot{\theta} \sin \theta + 2gl \sin \theta = 0 \end{aligned}$$

$$= 2l\ddot{\theta} + 4l\dot{\theta} + 2\ddot{x} \cos \theta + 2g \sin \theta = 0$$

$$= l\ddot{\theta} + 2l\dot{\theta} + \ddot{x} \cos \theta + g \sin \theta = 0$$

The equation of motion of the crane model associated with the generalized coordinates $\bar{q} = \{x, \theta\}$ can be summarized, respectively as:

$$x: F_x = (M + m)\ddot{x} + ml(\ddot{\theta} \cos \theta - \dot{\theta}^2 \sin \theta) + 2m\dot{l}\dot{\theta} \cos \theta + m\ddot{l} \sin \theta$$

$$\theta: l\ddot{\theta} + 2\dot{l}\dot{\theta} + \ddot{x} \cos \theta + g \sin \theta = 0$$

4.2 Linearization of the System

The above derived model is a nonlinear model. The nonlinear model has to be linearized to simplify the progress of the modeling. For safe operation, two assumptions had been made. First, we assume that the swing angle should be kept small

$$\theta \approx 0$$

$$\dot{\theta} \approx 0$$

In this study, we assume that changing the rope length is needed only to avoid obstacles in the path of the load. This change can be considered small too.

$$\dot{l} \approx \ddot{l} \approx 0$$

Using these two assumptions, the simplified equation of motion for the gantry crane system can be obtained

$$x: F_x = (M + m)\ddot{x} + ml\ddot{\theta}$$

$$\theta: l\ddot{\theta} + \ddot{x} + g\theta = 0$$

4.3 General State-space Representation of the System

After getting the linearized equation, equation can be written in state representation

$$\dot{x} = Ax + Bu$$

Where,

$$x = \begin{bmatrix} x \\ \theta \\ \dot{x} \\ \dot{\theta} \end{bmatrix} \quad \dot{x} = \begin{bmatrix} \dot{x} \\ \dot{\theta} \\ \ddot{x} \\ \ddot{\theta} \end{bmatrix}$$

From equation (3.9),

$$\ddot{x} = -l\ddot{\theta} - g\theta$$

Substituting equations will get the following equation,

$$F_x = (M + m)(-l\ddot{\theta} - g\theta) + ml\ddot{\theta}$$

$$\ddot{\theta} = -\left[\left(\frac{M + m}{Ml}\right)g\theta + \frac{F_x}{Ml}\right]$$

Substitute above equations

$$F_x = (M + m)(-l\ddot{\theta} - g\theta) - ml\left[\left(\frac{M + m}{Ml}\right)g\theta + \frac{F_x}{Ml}\right]$$

$$\ddot{x} = \frac{F_x}{M} + \left(\frac{m}{M}\right)g\theta$$

Equations can be arranged into the matrix form as below:

$$\begin{bmatrix} \dot{x} \\ \dot{\theta} \\ \ddot{x} \\ \ddot{\theta} \end{bmatrix} = \begin{bmatrix} 0 & 0 & 1 & 0 \\ 0 & 0 & 0 & 1 \\ 0 & \frac{mg}{M} & 0 & 0 \\ 0 & -\frac{(M + m)}{Ml} & 0 & 0 \end{bmatrix} \begin{bmatrix} x \\ \theta \\ \dot{x} \\ \dot{\theta} \end{bmatrix} + \begin{bmatrix} 0 \\ 0 \\ \frac{1}{M} \\ -\frac{1}{Ml} \end{bmatrix} F_x$$

The output equation is

$$\begin{bmatrix} x \\ \theta \end{bmatrix} = \begin{bmatrix} 1 & 0 & 0 & 0 \\ 1 & 0 & 0 & 0 \end{bmatrix} \begin{bmatrix} x \\ \theta \\ \dot{x} \\ \dot{\theta} \end{bmatrix}$$

4.4 Transfer Function of 2D Crane System

The equations of motion for a linearized model of a 2D Crane are represented as follows:

$$F_x = (m_1 + m_2)\ddot{x} + m_2 l \ddot{\theta} \quad (1)$$

$$l \ddot{\theta} + \dot{x} + g \theta = 0 \quad (2)$$

From equation (2)

$$\ddot{x} = -l \ddot{\theta} - g \theta \quad (3)$$

Representation of Models in Laplace or S Domain

In order to represent the Equations (5) and (7) in s domain, their respective transfer functions can be derived through Laplace transformation assuming the initial states to be zero. Thus for Equation (5), it becomes:

$$F_x(s) = (m_1 + m_2)s^2 X(s) + m_2 l s^2 \theta(s) \quad (4)$$

Equation (2) become

$$l s^2 \theta(s) + s^2 X(s) + g \theta(s) = 0 \quad (5)$$

Rearranging equation (5), we get:

$$\theta(s) = \frac{-s^2 X(s)}{l s^2 + g} \quad (6)$$

And

$$X(s) = \left[\frac{-l s^2 \theta(s) - g \theta(s)}{s^2} \right] \quad (7)$$

Substituting Equation (6) into Equation (4), a transfer function is obtained as follows:

$$\frac{X(s)}{F_x(s)} = \frac{l s^2 + g}{m_1 l s^4 + s^2 g (m_1 + m_2)} \quad (8)$$

Similarly, substituting Equation (7) into Equation (4), another transfer function is derived as follows:

$$\frac{\theta(s)}{F_x(s)} = \frac{1}{-m_1 l s^2 - (m_1 + m_2)g} \quad (9)$$

4.5 Dynamic Behaviors Simulation of 2D Crane

Figure 6 below shows the block diagram of 2D Crane system that is used to simulate the dynamic behavior of the 2D Crane system in this project. As mentioned above, the gantry crane system is represented by the Differential Equation Editor, DEE tool.

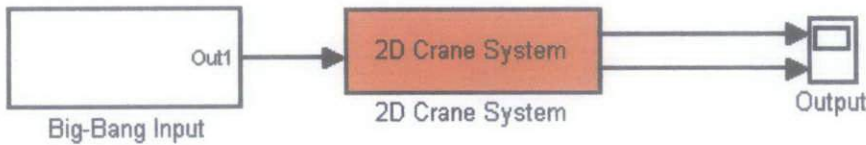


Figure 6.1: 2D Crane

The input to the 2D Crane system is a bang-bang torque. The bang-bang input force is generated using the multiple unit step input.

Figure 6 shows the general PID Controller for 2D Crane System that will be used to obtain the maximum performance of 2D Crane System. Three scopes are used to capture the trolley position and sway angle.

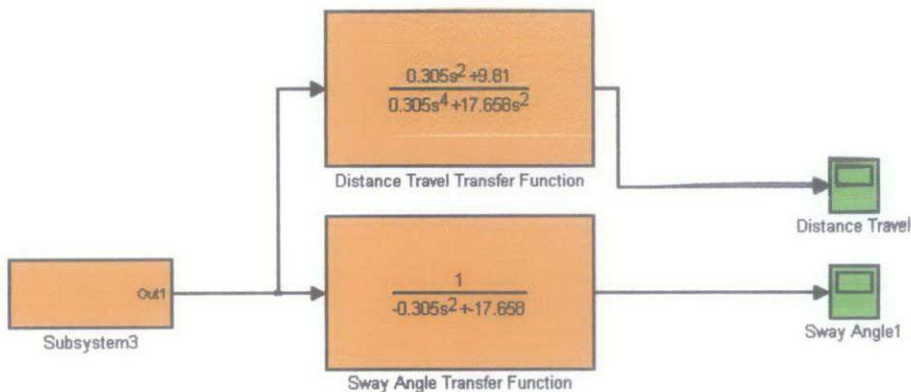


Figure 6.2: PID Controller for 2D Crane

Figure 7 shows the Differential Equation Editor, DEE box where the state space equation for 2D Crane Dynamics are entered for simulation purposes.

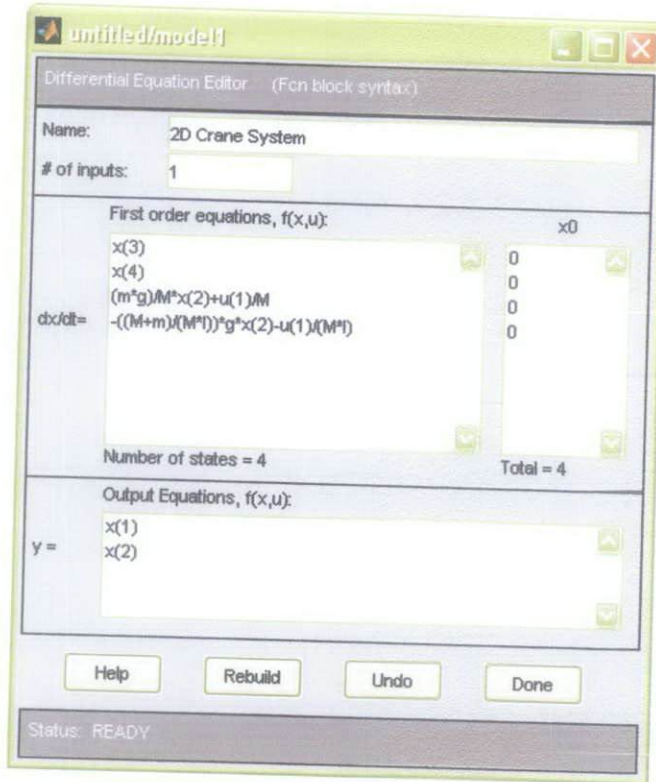


Figure 7: DEE for 2D Crane System

Using the control system toolbox in Matlab, the controllability and observability of the system is being analyzed. Using the matrix method, the state space equation of the 2D Crane system is obtained and ranked. Based on the results obtained, the state space equation of the 2D Crane System is controllable and observable.

4.6 Sway Motion of 2D Crane

Figures show the sway angle of the 2D crane, θ when input force, F is applied to the trolley. The initial position is assumed to have a sway angle of zero since no force is applied to the trolley. When a positive force is applied to the trolley as showed in Figure 8, the payload will swing clock wise direction. The sway angle will be a negative value. However, the payload will swing anticlockwise direction when the input force is negative as showed in Figure 10 and the sway angle will be a positive value.

In simulation using Matlab/Simulink Software for the project, the following 2D Crane parameters are used:

Trolley mass, $M = 1 \text{ kg}$

Payload mass, $m = 0.8 \text{ kg}$

Length of hoisting rope, $l = 0.305 \text{ m}$

Gravity, $g = 9.81 \text{ m/s}^2$

Input force, $F = 1 \text{ N}$

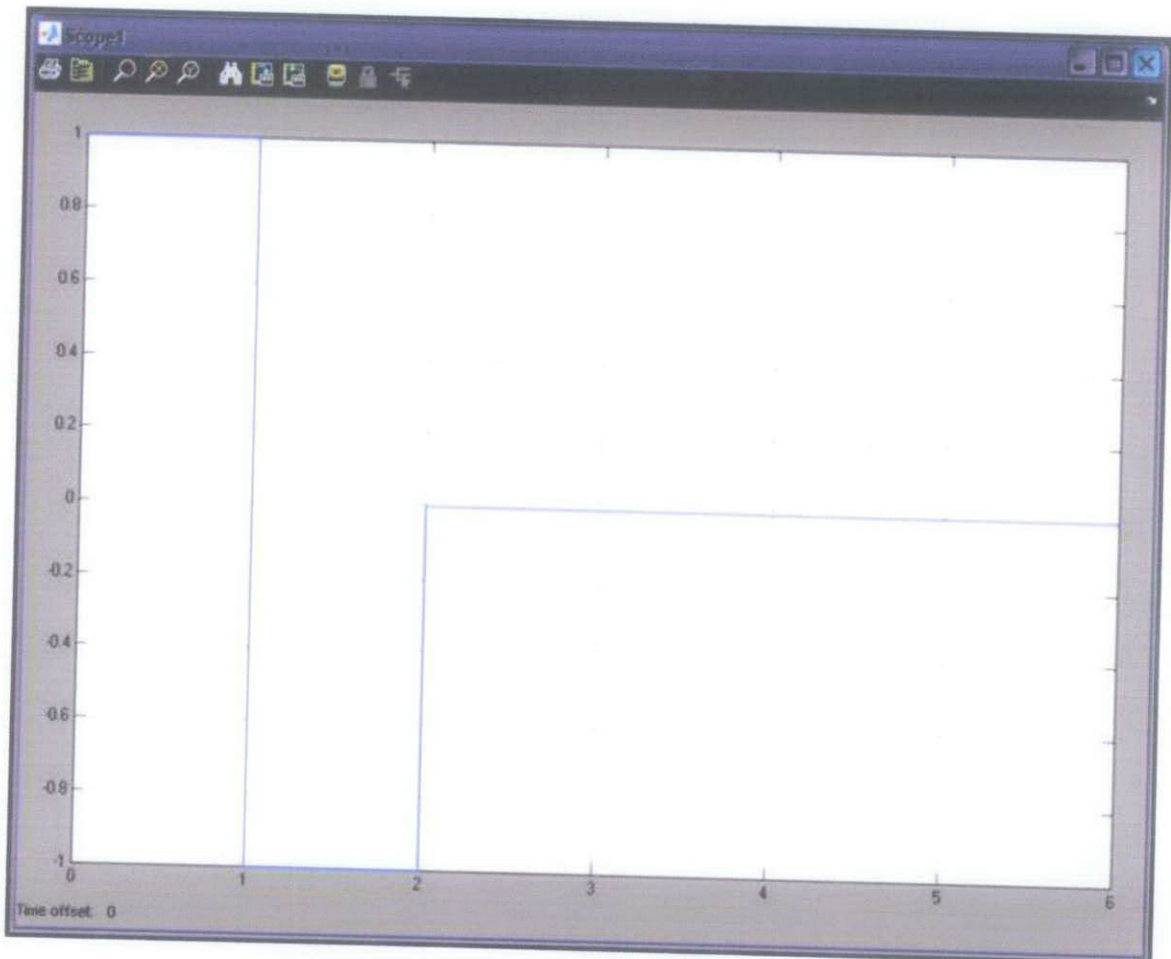


Figure 8: Bang-bang Input Force, 1N

When input force is applied to the trolley, the trolley will travel horizontally along its path. Graph above shows that the trolley reached around 0.58 at 2s. The input force will be taken away after 2s. The oscillation after 2s is due to the non-stop oscillation of the payload.

4.7 Trolley Position

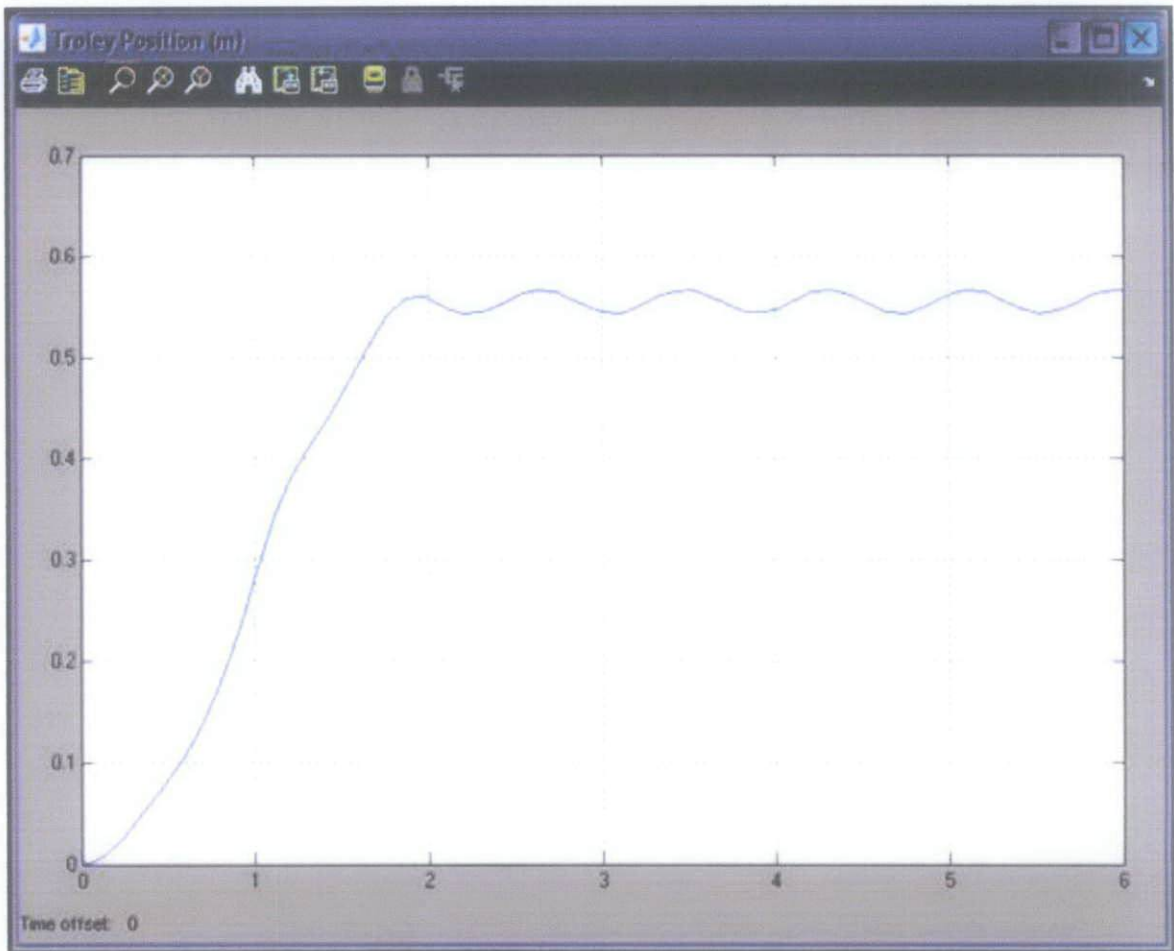


Figure 9: Trolley Position (m)

Due to the force applied to the 2D Crane System, the trolley moved accordingly to its position. Based on the Figure 9 above, the trolley position reach a constant value under 2s period. The final value of trolley position is 0.55m in average.

4.8 Sway Angle

Due to the positive input force applied, the payload swing at a clockwise direction at the starting of the simulation. The payload will continue to oscillate although the force is taken off after 2s. This is because the 2D Crane system is designed without sway angle damper.

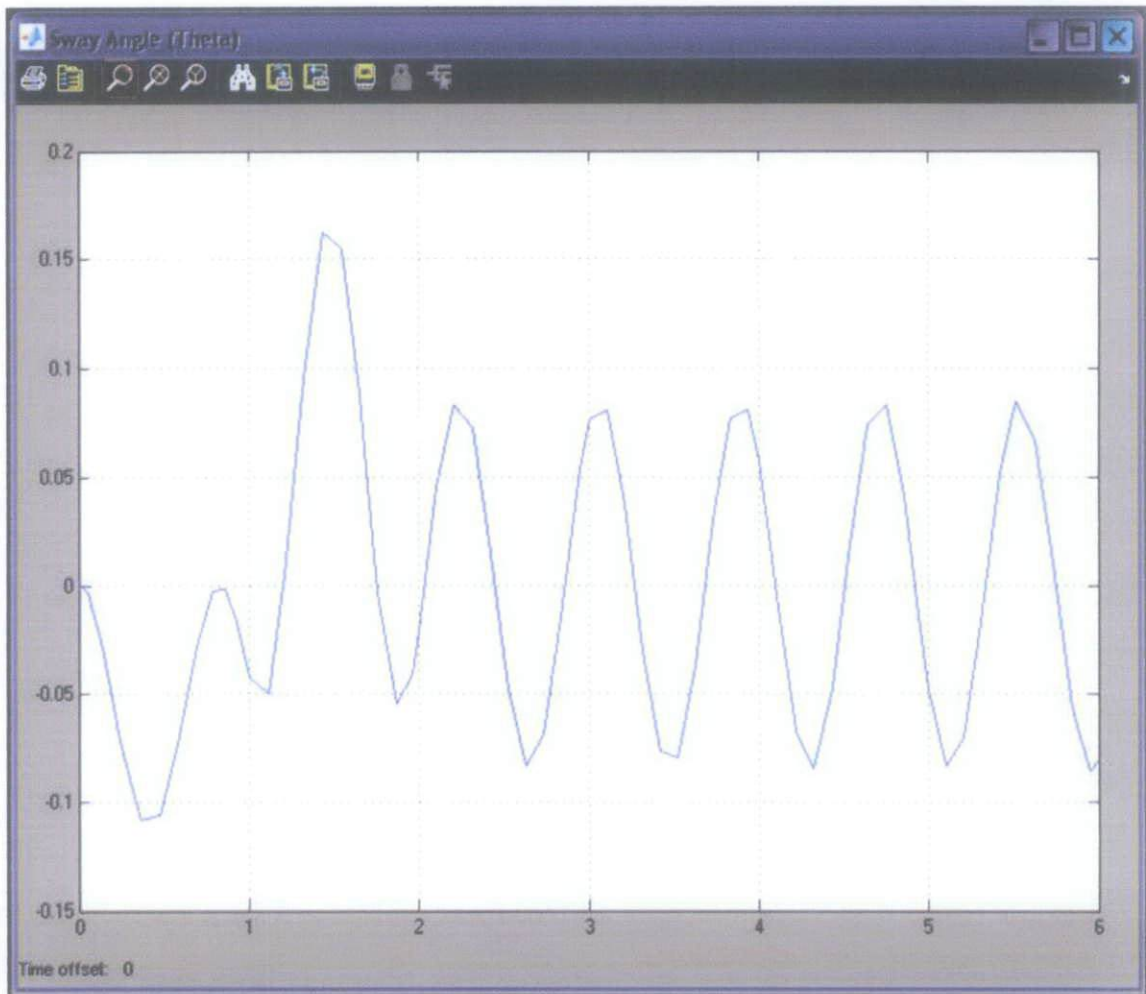


Figure 10: Sway Angle (rad)

4.9 System Analysis and Discussion

The effect of input force, length of the hoisting rope, trolley mass and payload mass on the dynamic behavior of the gantry crane are investigated. By changing the system parameters such as payload mass (m), trolley mass (M), length of the hoisting rope (l) and the input force (F), the dynamic performance of the gantry crane will be affected. The swing magnitude and the travelling distance will change when the system parameters changed.

4.9.1 Input Force, F

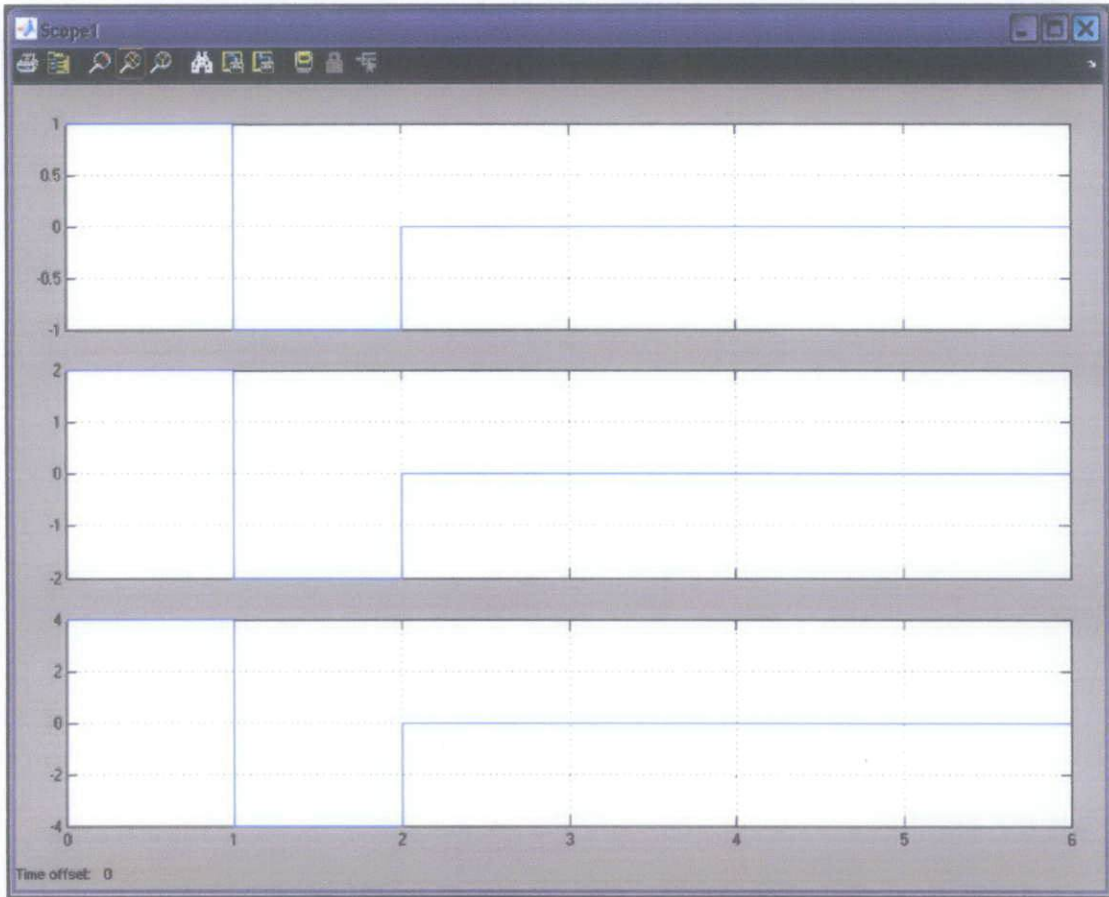


Figure 11: Bang-bang Input Force at 1N, 2N and 4N

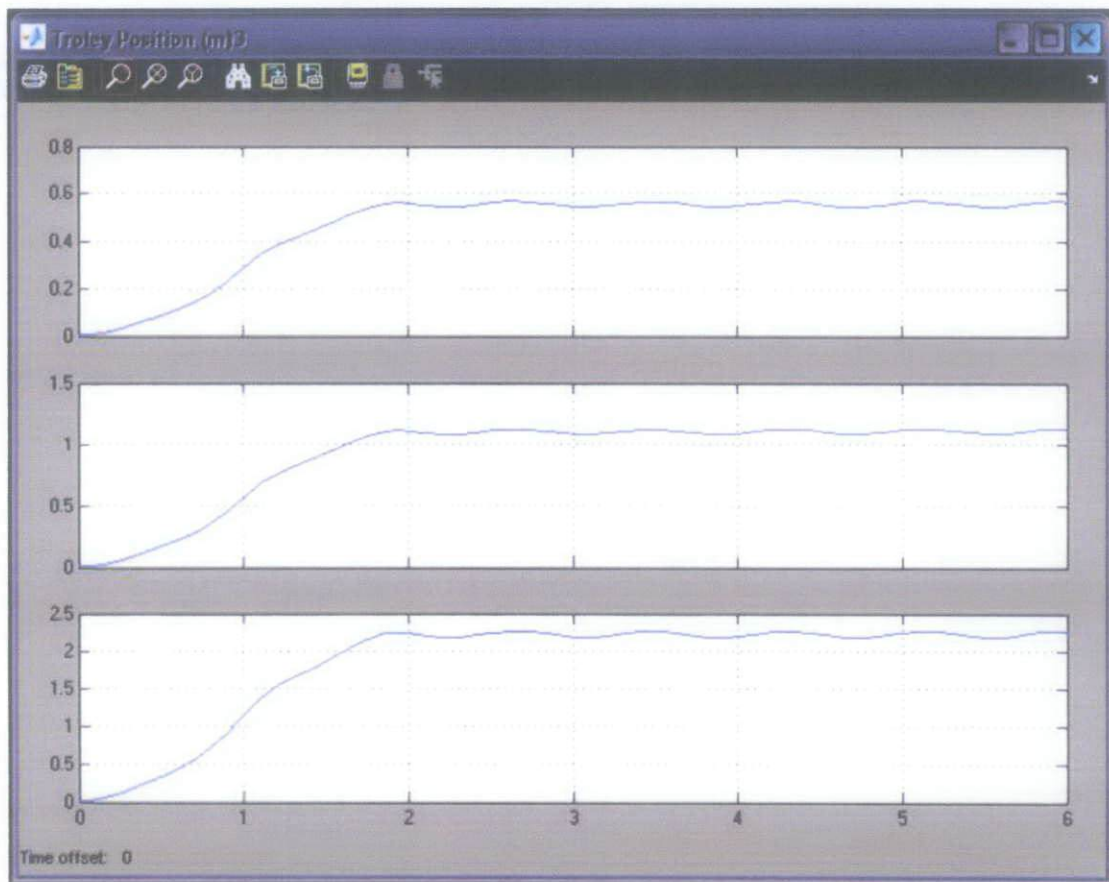


Figure 12: Trolley Position for Force at 1N, 2N and 4N

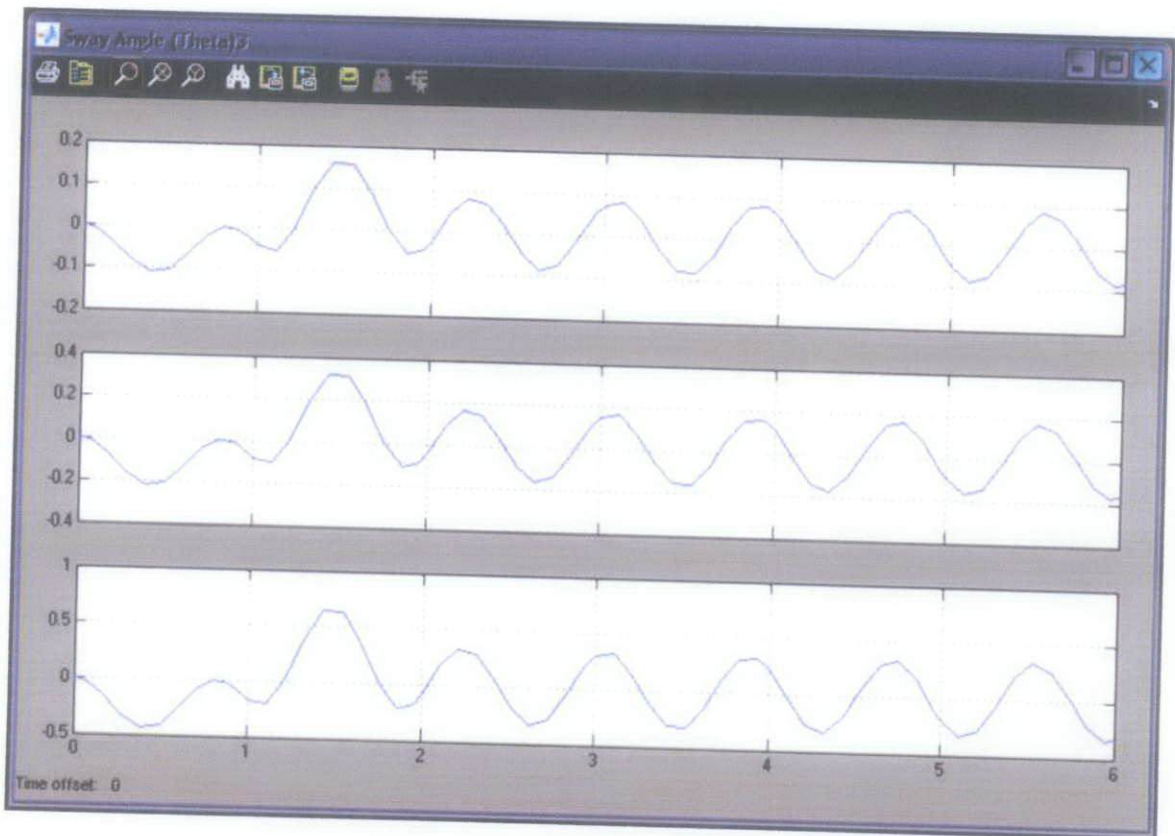


Figure 13: Sway Angle for Force at 1N, 2N and 4N

Figure 11 shows the different input force that applied to the system. Figure 12 and 13 show the responses of the system in term of trolley position and sway angle when different input force applied to the system.

From the graph obtain, as we increases the amount of torque or force to the system, the travel distance of the trolley will increases but at the same time, the sway angle will increase thus affecting the system reliability. Besides that, we also observe that the sway frequency of the payload remain the same for different amount of force applied. By applying the **PID Controller** in the future, it was hope that the amount of sway angle will decrease or able to damped the sway angle over time.

When the input force is 4N, the trolley is able to travel more distance where it can reaches around 2.25m from its initial position. However the vibration of the trolley is higher which has a maximum magnitude of around 0.6 rad as the sway angle frequency remains the same.

4.9.2 Length of Hoisting Rope, l

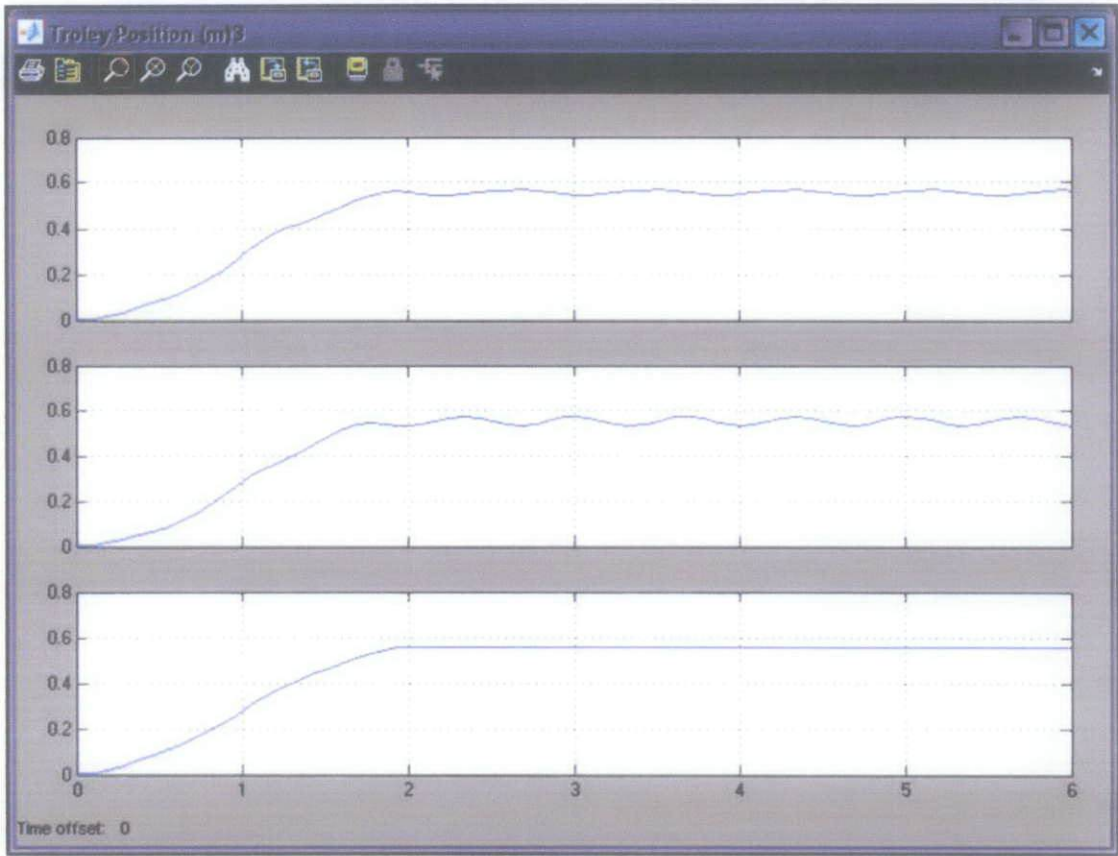


Figure 14: Trolley Position for Hoisting Rope length, l of 0.305m, 0.2m and 0.5m

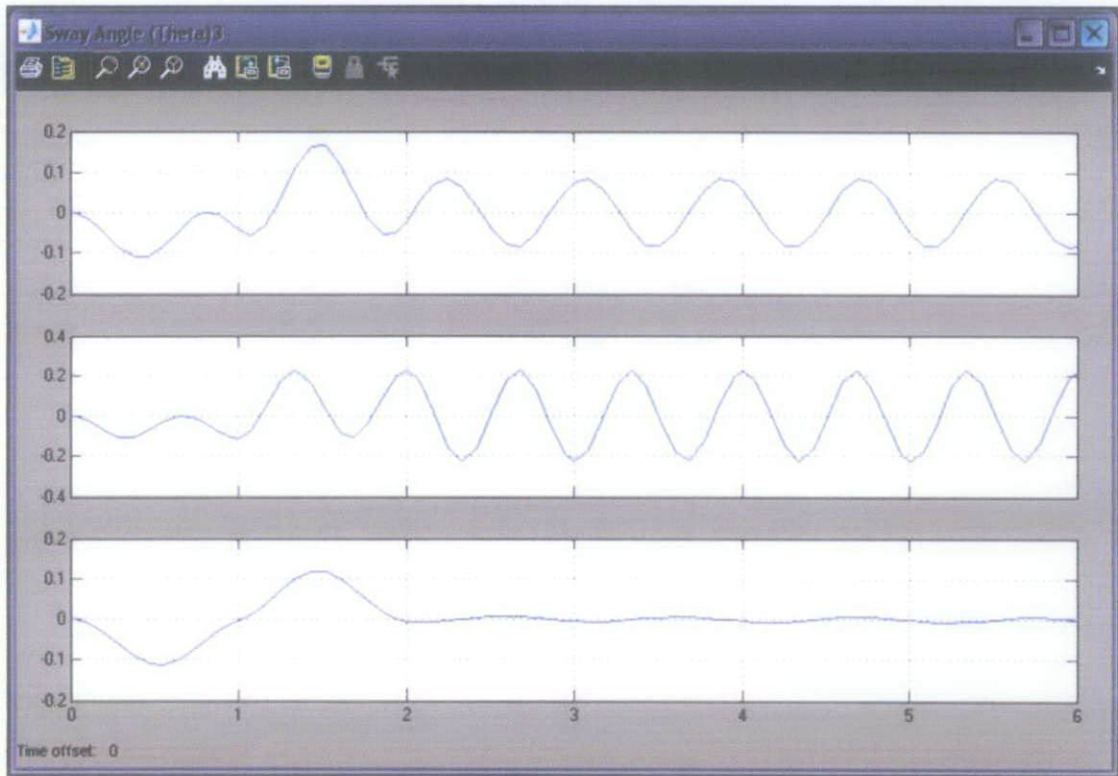


Figure 15: Sway Angle for Hoisting Rope length, l of 0.305m, 0.2m and 0.5m

Trolley still reaches the same distance since the same force of 1N is applied to the system. Thus, in general, the length of the hoisting rope does not affect the distance travel by the trolley. However, as we decreased the length of the hoisting rope, the fluctuation of the trolley increased, this due to the payload oscillation increased when the rope is shorter. From the Figure 15, the magnitude and frequency of the payload swing can be observed to be greater.

From Figure 15, we can observe that as we increase the value of hoisting rope, l to 0.5 m, the payload sway angle stabilized after 2 s. In conclusion, the length of hoisting rope, l needs to be controlled in order to obtain the maximum reliability of the 2D Crane System since with the lower or smaller oscillation of the payload, the trolley can reach the same location but more stable sway angle.

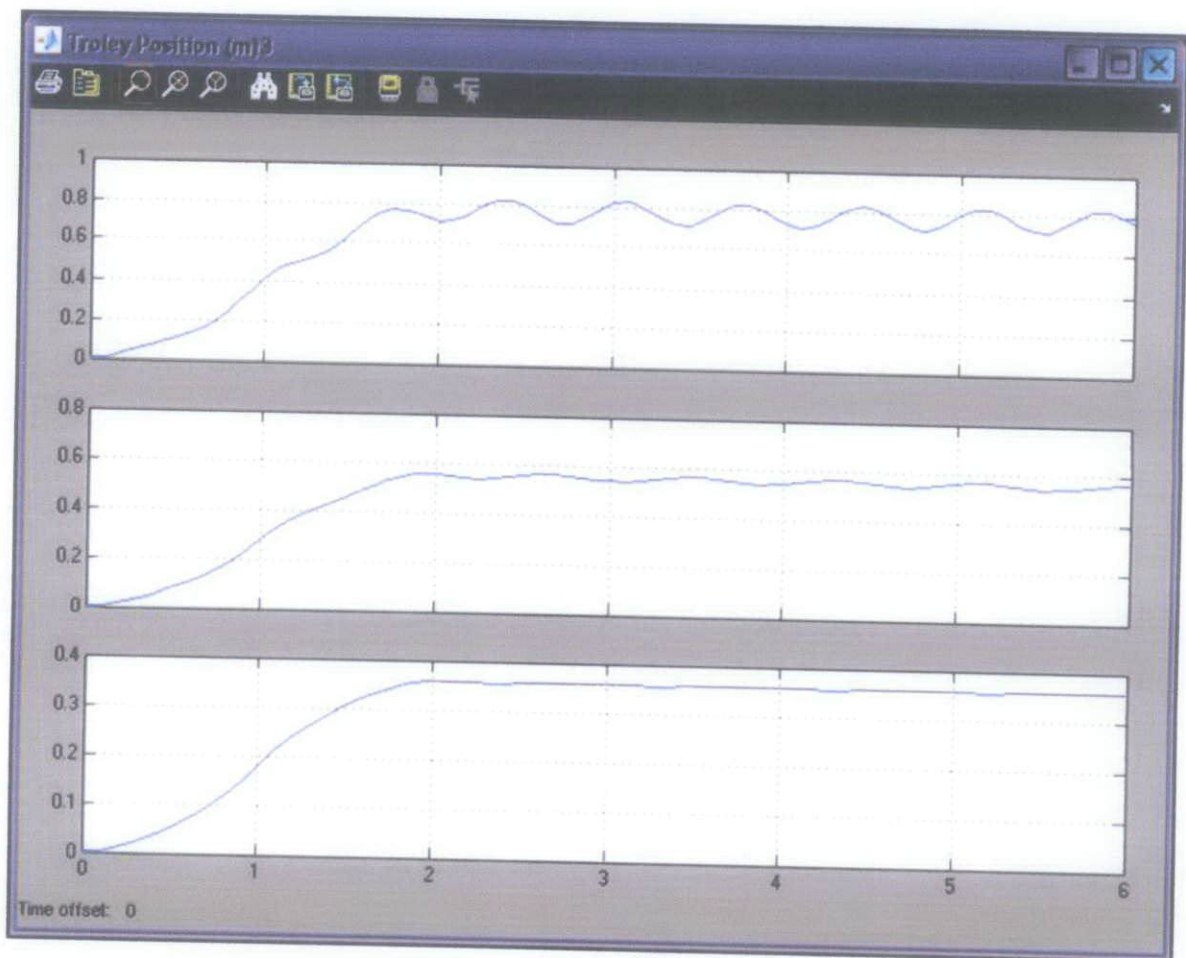


Figure 16: Trolley Position for Trolley Mass, M of 0.5 kg, 1 kg and 2 kg

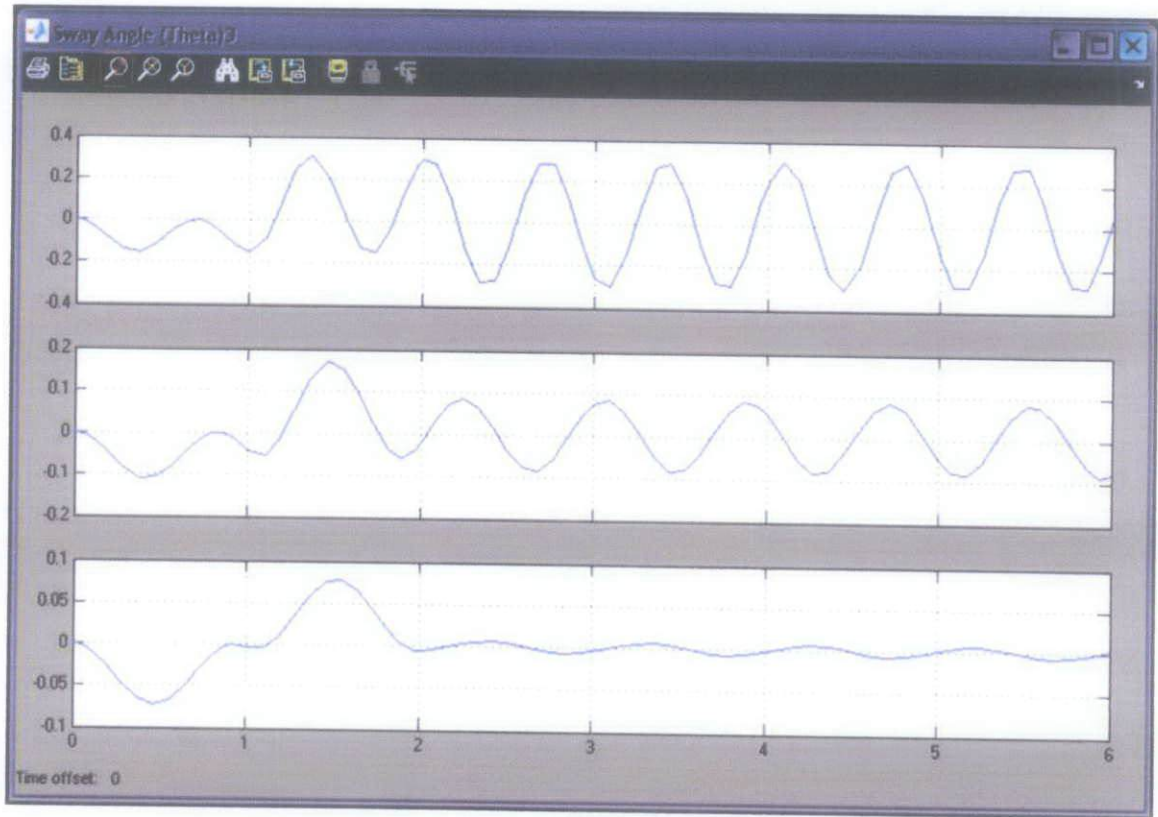


Figure 17: Sway Angle for Trolley Mass, M of 0.5 kg, 1 kg and 2 kg

Based on the figures above, when the trolley mass, M increases from 0.5 kg to 2 kg, the magnitude and frequency of the payload swing decrease. From Figure 16, the smaller trolley mass which is 0.5 kg will travel a greater distance compared to the highest trolley mass 2 kg, this is due to the gravitational force that absorbed the force applied to move the system.

In conclusion, as the trolley mass, M increases, the distance travelled by the trolley will decrease. Besides that, it will also result in a lower magnitude, fluctuation and frequency of the payload swing which will result in a more reliable 2D Crane System.

4.9.3 Payload Mass, m

Finally, the effect on the trolley position and payload sway angle by payload mass, m . This is important to determine the maximum and minimum limit of payload mass that can be used for the 2D System created.

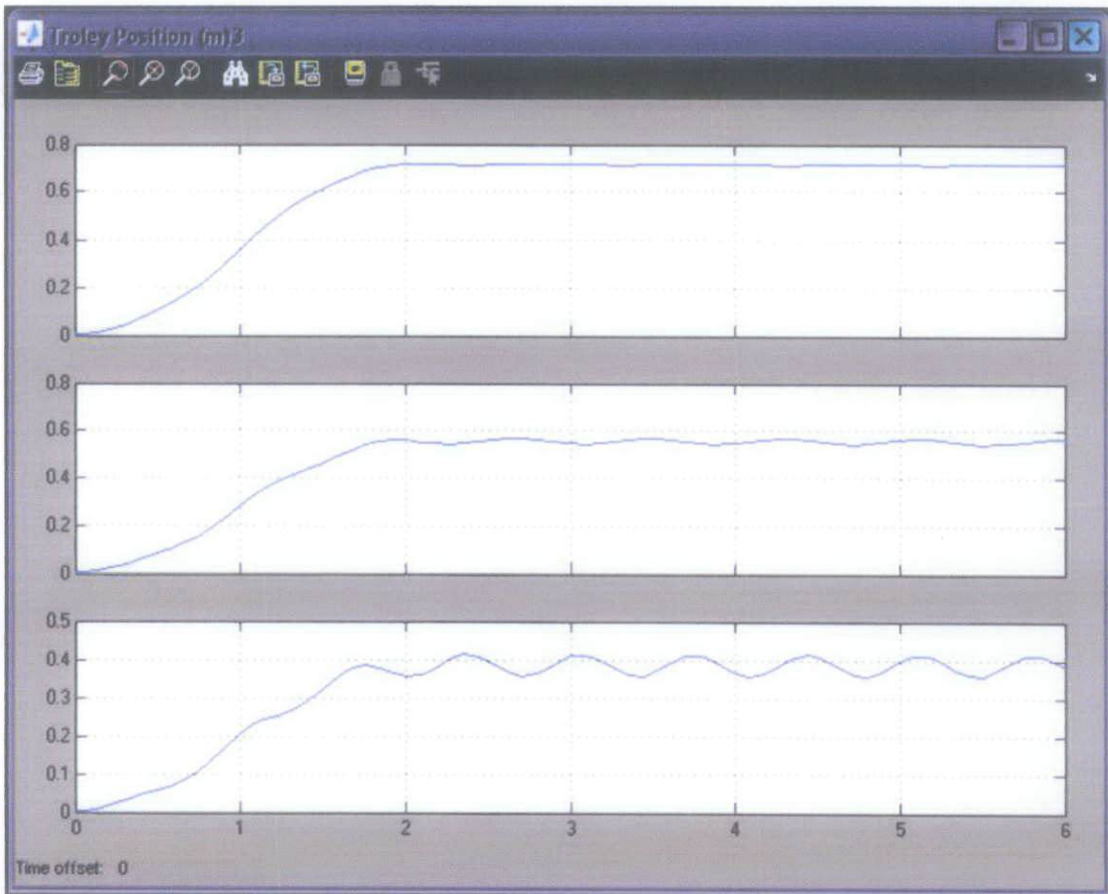


Figure 18: Trolley Position for Payload Mass, M of 0.4 kg, 0.8 kg and 1.6 kg

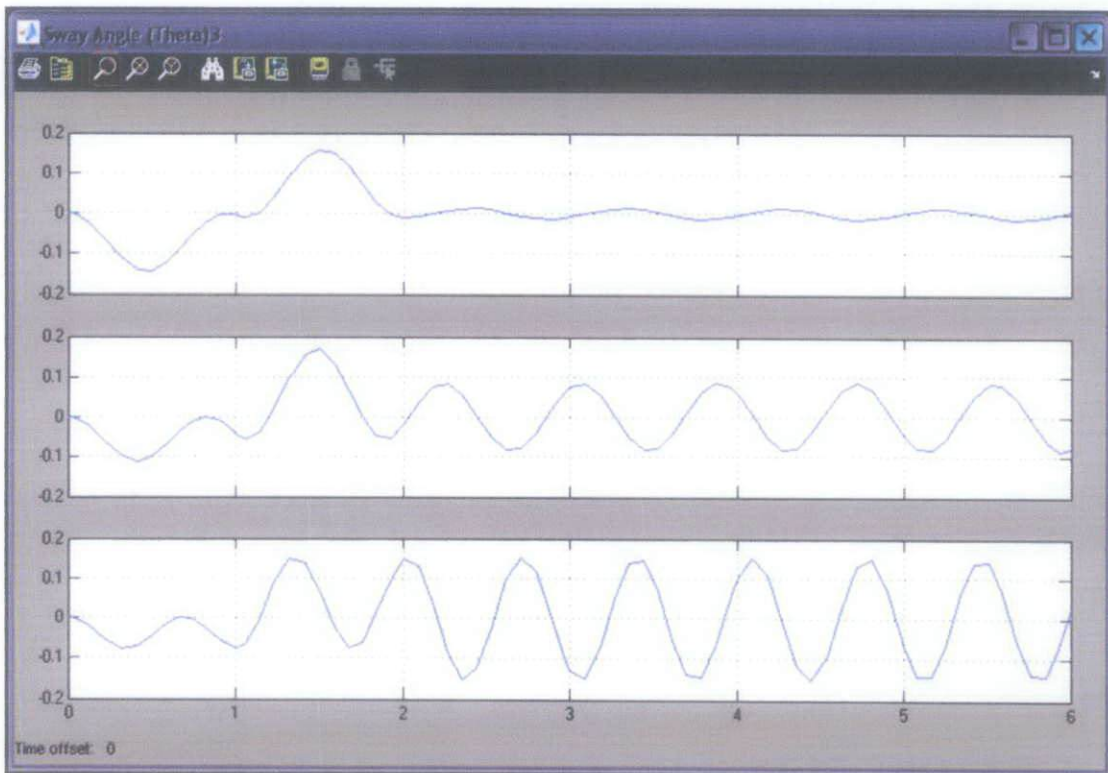


Figure 19: Sway Angle for Payload Mass, M of 0.4 kg, 0.8 kg and 1.6 kg

Figure 18 and 19 shows the performance of the 2D Crane System when we increase and decrease the payload mass, m . When payload mass is increase from 0.4 kg to 1.6 kg, the trolley position increased but the payload sway angle decreased. Thus in general, the reliability of the 2D Crane System will increased as the payload mass decreased.

4.10 Simulation of 2D Crane Using Transfer Function

Using the transfer function obtained earlier, the differential equation of the 2D Crane is replaced with the transfer function. This is important to verify the results obtained by using the differential equation approach earlier. Figure 20 shows the block diagram of 2D Crane system that is used to simulate the dynamic behavior of the 2D Crane system using transfer function approach. In simulation using Matlab/Simulink Software for the project, the same 2D Crane parameters are used:-

Trolley mass, $M = 1$ kg

Payload mass, $m = 0.8$ kg

Length of hoisting rope, $l = 0.305$ m

Gravity, $g = 9.81$ m/s²

Input force, $F = 1$ N

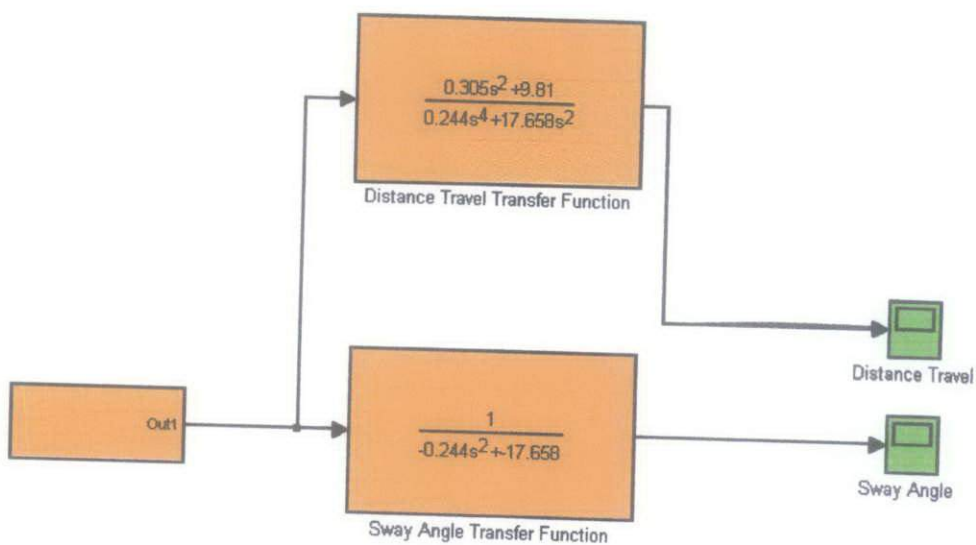


Figure 20: Block Diagram of 2D Crane System

As shown in the Figure 20, the linear value of the 2D Crane is substituted into the 2D Crane System to obtain the transfer function of both distance travelled and sway angle:-

$$\frac{X(s)}{F_x(s)} = \frac{ls^2 + g}{m_1ls^4 + s^2g(m_1 + m_2)} = \frac{0.305s^2 + 9.81}{0.244s^4 + 17.658s^2}$$

$$\frac{\theta(s)}{F_x(s)} = \frac{1}{-m_1ls^2 - (m_1 + m_2)g} F_x(s) = \frac{1}{-0.244s^4 - 17.658s^2}$$



Figure 21: Trolley Position (m)

Figure 21 is the output graph for trolley position of the 2D Crane. Based on the figure, we conclude that the transfer function system behave the same way as the differential equation method. The oscillation for transfer function method is higher compare to the differential equation method but based on the distance travelled by the trolley we conclude that the result for both methods will produce the same average travelled distance which is 0.6m.

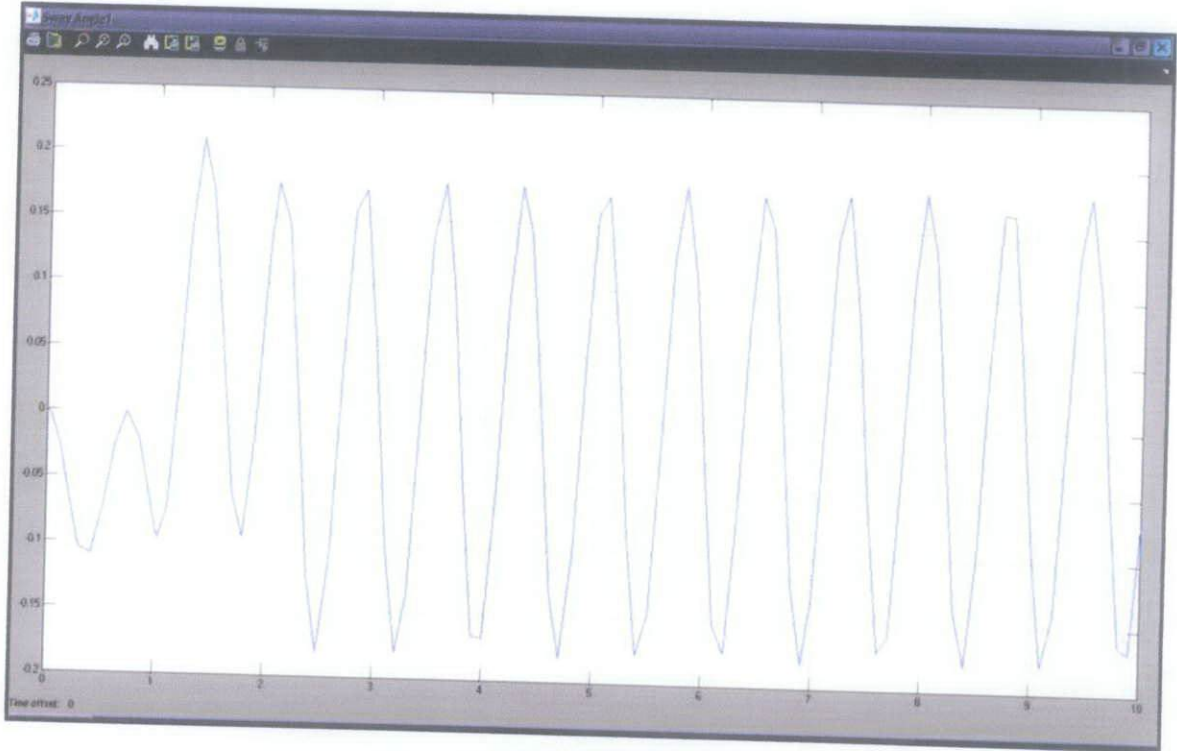


Figure 22: Sway Angle (rad)

Figure 22 shows the sway angle output produced using the 2D Crane system transfer function. Based on the graph produced, we concluded that the sway angle for transfer function method is higher compare to the differential equation method. The oscillation for both sway angle and trolley position is higher compare to the differential equation method. The deviation may be cause by the 3 decimal point value substituted into the equation of transfer function for calculation.

4.11 Formulation of 2D Crane Using State-space Approach

Using a state variable approach gives a straightforward way to analyze a single-input single-output (SISO) and a multiple input, multiple-output (MIMO) system. The state model constructed from transfer functions are not unique and can have different forms. There are two approaches that are used for this project which is control canonical form and observer canonical form. Each approach will result in a different form of state model.

Using the results of 2D Crane System transfer function obtained earlier, the state-space equation of the 2D Crane is obtained. This is important to verify the results obtained by using the differential equation and transfer function approach earlier. Figure 23 shows the block diagram of 2D Crane system that is used to simulate the dynamic behavior of the 2D Crane system using transfer function approach.

In simulation using Matlab/Simulink Software for the project, the same 2D Crane parameters are used:-

Trolley mass, $M = 0.8$ kg

Payload mass, $m = 1$ kg

Length of hoisting rope, $l = 0.305$ m

Gravity, $g = 9.81$ m/s²

Input force, $F = 1$ N

4.11.1 Control Canonical Form of 2D Crane System

$$\frac{X(s)}{F_x(s)} = \frac{ls^2 + g}{m_1ls^4 + s^2g(m_1 + m_2)} = \frac{\beta_2s^2 + \beta_0}{\alpha_4s^4 + \alpha_2s^2}$$

$$\frac{\theta(s)}{F_x(s)} = \frac{1}{-m_1ls^2 - (m_1 + m_2)g} F_x(s) = \frac{\beta_0}{\alpha_2s^2 + \alpha_0}$$

From the transfer function above, the similarities for both equations is defined. Thus, the new equation of transfer function is produced. Which is:-

$$\frac{X(s)}{F_x(s)} = \frac{-ls^2 - g}{-m_1ls^4 - s^2g(m_1 + m_2)} = \frac{\beta_2s^2 + \beta_0}{\alpha_4s^4 + \alpha_2s^2}$$

$$\frac{\theta(s)}{F_x(s)} = \frac{s^2}{-m_1ls^4 - s^2g(m_1 + m_2)} F_x(s) = \frac{\beta_2s^2}{\alpha_4s^4 + \alpha_2s^2}$$

Based on the variables assigned, the corresponding signal graph are obtained and applied into the Matlab/Simulink for simulation. The results of the simulation are

compared to the previous method in order to verify the accuracy of the signal graph produced. Figure 23 below shows the block diagram constructed from the signal flow graph obtained earlier.

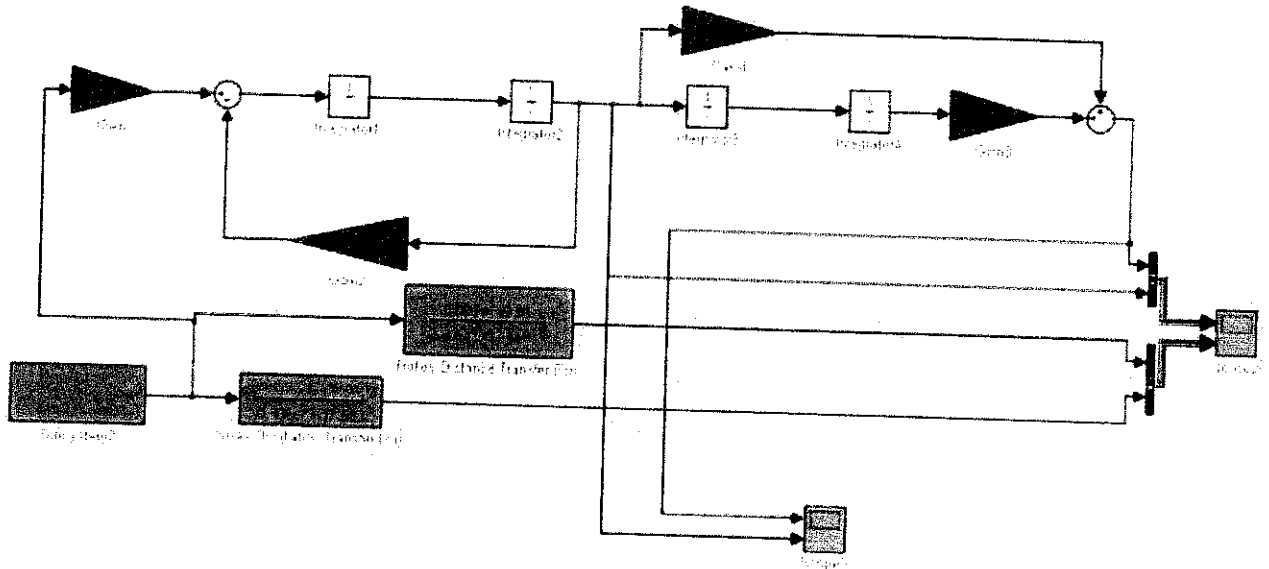


Figure 23: Signal Flow Graph Block Diagram for 2D Crane

Control Canonical Form in Matrix Form (2D Crane)

$$\begin{bmatrix} \dot{x}_1 \\ \dot{x}_2 \\ \dot{x}_3 \\ \dot{x}_4 \end{bmatrix} = \begin{bmatrix} 0 & 1 & 0 & 0 \\ 0 & 0 & 1 & 0 \\ 0 & 0 & 0 & 1 \\ 0 & 0 & \frac{(m_1 + m_2)g}{-m_1 l} & 0 \end{bmatrix} \begin{bmatrix} x_1 \\ x_2 \\ x_3 \\ x_4 \end{bmatrix} + \begin{bmatrix} 0 \\ 0 \\ 0 \\ -m_1 l \end{bmatrix} [u]$$

$$\begin{bmatrix} y_1 \\ y_2 \end{bmatrix} = \begin{bmatrix} -g & 0 & -1 & 0 \\ 0 & 0 & 1 & 0 \end{bmatrix} \begin{bmatrix} x_1 \\ x_2 \\ x_3 \\ x_4 \end{bmatrix}$$

Substituting values into the Matrix

$$\begin{bmatrix} \dot{x}_1 \\ \dot{x}_2 \\ \dot{x}_3 \\ \dot{x}_4 \end{bmatrix} = \begin{bmatrix} 0 & 1 & 0 & 0 \\ 0 & 0 & 1 & 0 \\ 0 & 0 & 0 & 1 \\ 0 & 0 & -72.369 & 0 \end{bmatrix} \begin{bmatrix} x_1 \\ x_2 \\ x_3 \\ x_4 \end{bmatrix} + \begin{bmatrix} 0 \\ 0 \\ 0 \\ -0.244 \end{bmatrix} [u]$$

$$\begin{bmatrix} y_1 \\ y_2 \end{bmatrix} = \begin{bmatrix} -9.81 & 0 & -1 & 0 \\ 0 & 0 & 1 & 0 \end{bmatrix} \begin{bmatrix} x_1 \\ x_2 \\ x_3 \\ x_4 \end{bmatrix}$$

4.11.2 Observer Canonical Form of 2D Crane System

In obtaining the state-space representation of observer canonical form of the 2D Crane System, the concept of duality is used. Since the value of the β will be varied thus the input of the system will be different. For different input to obtain a different output, both outputs are separated into two different control canonical equations. Below are the steps involved:-

Renumbering in reverse order

$$\begin{bmatrix} \dot{x}_4 \\ \dot{x}_3 \\ \dot{x}_2 \\ \dot{x}_1 \end{bmatrix} = \begin{bmatrix} 0 & 1 & 0 & 0 \\ 0 & 0 & 1 & 0 \\ 0 & 0 & 0 & 1 \\ 0 & 0 & \frac{(m_1 + m_2)g}{-m_1 l} & 0 \end{bmatrix} \begin{bmatrix} x_4 \\ x_3 \\ x_2 \\ x_1 \end{bmatrix} + \begin{bmatrix} 0 \\ 0 \\ 0 \\ 1 \\ -m_1 l \end{bmatrix} [u]$$

$$\begin{bmatrix} y_2 \\ y_1 \end{bmatrix} = \begin{bmatrix} -g & 0 & -1 & 0 \\ 0 & 0 & 1 & 0 \end{bmatrix} \begin{bmatrix} x_4 \\ x_3 \\ x_2 \\ x_1 \end{bmatrix}$$

Rearranging in ascending numerical order

$$\begin{bmatrix} \dot{x}_1 \\ \dot{x}_2 \\ \dot{x}_3 \\ \dot{x}_4 \end{bmatrix} = \begin{bmatrix} 0 & \frac{(m_1 + m_2)g}{-m_1 l} & 0 & 0 \\ 1 & 0 & 0 & 0 \\ 0 & 1 & 0 & 0 \\ 0 & 0 & 1 & 0 \end{bmatrix} \begin{bmatrix} x_1 \\ x_2 \\ x_3 \\ x_4 \end{bmatrix} + \begin{bmatrix} 1 \\ -m_1 l \\ 0 \\ 0 \\ 0 \end{bmatrix} [u]$$

$$\begin{bmatrix} y_1 \\ y_2 \end{bmatrix} = \begin{bmatrix} 0 & 1 & 0 & 0 \\ 0 & -1 & 0 & -g \end{bmatrix} \begin{bmatrix} x_1 \\ x_2 \\ x_3 \\ x_4 \end{bmatrix}$$

After rearranging the matrix in ascending order, the transpose matrix are obtained based on the steps below:-

$$A_c = A^T; B_c = C^T; C_c = B^T; D_c = D^T$$

$$X = Ax + Bu; Y = Cx + Du$$

Sway Angle Observer Canonical Form

$$\begin{bmatrix} \dot{x}_1 \\ \dot{x}_2 \\ \dot{x}_3 \\ \dot{x}_4 \end{bmatrix} = \begin{bmatrix} 0 & 1 & 0 & 0 \\ (m_1 + m_2)g & 0 & 1 & 0 \\ -m_1 l & 0 & 0 & 1 \\ 0 & 0 & 0 & 0 \end{bmatrix} \begin{bmatrix} x_1 \\ x_2 \\ x_3 \\ x_4 \end{bmatrix} + \begin{bmatrix} 0 \\ 1 \\ 0 \\ 0 \end{bmatrix} [u]$$

$$[y_1] = \begin{bmatrix} 1 \\ -m_1 l & 0 & 0 & 0 \end{bmatrix} \begin{bmatrix} x_1 \\ x_2 \\ x_3 \\ x_4 \end{bmatrix}$$

Trolley Distance Observer Canonical Form

$$\begin{bmatrix} \dot{x}_1 \\ \dot{x}_2 \\ \dot{x}_3 \\ \dot{x}_4 \end{bmatrix} = \begin{bmatrix} 0 & 1 & 0 & 0 \\ (m_1 + m_2)g & 0 & 1 & 0 \\ -m_1 l & 0 & 0 & 1 \\ 0 & 0 & 0 & 0 \end{bmatrix} \begin{bmatrix} x_1 \\ x_2 \\ x_3 \\ x_4 \end{bmatrix} + \begin{bmatrix} 0 \\ -l \\ 0 \\ -g \end{bmatrix} [u]$$

$$[y_1] = \begin{bmatrix} 1 \\ -m_1 l & 0 & 0 & 0 \end{bmatrix} \begin{bmatrix} x_1 \\ x_2 \\ x_3 \\ x_4 \end{bmatrix}$$

The Signal Flow Graph can be obtained using methods shown in Figure 24 below:-

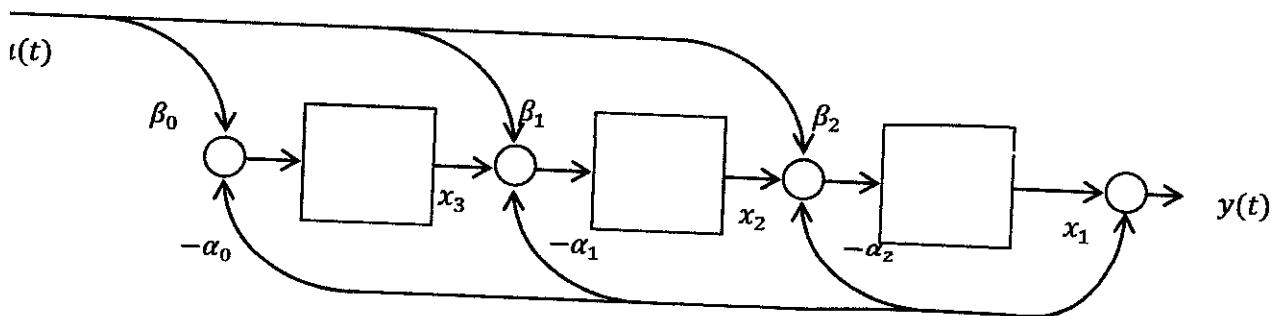


Figure 24: Signal Flow Graph of Observer Canonical Form

$$\begin{bmatrix} \dot{x}_1 \\ \dot{x}_2 \\ \dot{x}_3 \\ \dot{x}_4 \end{bmatrix} = \begin{bmatrix} -\alpha_3 & 1 & 0 & 0 \\ -\alpha_2 & 0 & 1 & 0 \\ -\alpha_1 & 0 & 0 & 1 \\ -\alpha_0 & 0 & 0 & 0 \end{bmatrix} \begin{bmatrix} x_1 \\ x_2 \\ x_3 \\ x_4 \end{bmatrix} + \begin{bmatrix} \beta_3 \\ \beta_2 \\ \beta_1 \\ \beta_0 \end{bmatrix} [u]; [y_1] = \begin{bmatrix} 1 \\ -m_1 l & 0 & 0 & 0 \end{bmatrix} \begin{bmatrix} x_1 \\ x_2 \\ x_3 \\ x_4 \end{bmatrix}$$



Figure 26: Trolley Position (m)

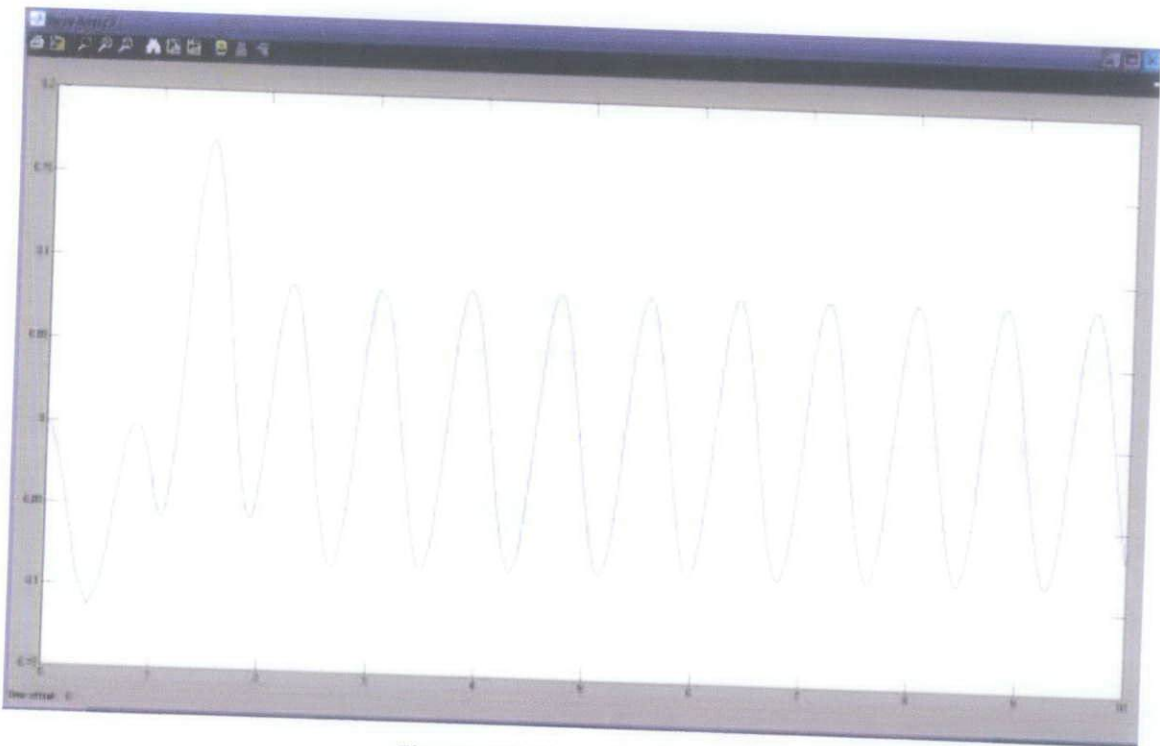


Figure 27: Sway Angle (rad)

Figure 26 is the output graph for trolley position of the 2D Crane. Based on the figure, we conclude that the state-space obtained behave the same way as the differential equation and transfer function method. The oscillation and value of trolley position is

exactly the same as the transfer function method thus we concluded that the signal flow graph used in this state-space approach is correct. In this project, the simulation are applied using control canonical form of state-space approach because we assumed that the other model such as observer canonical form will results in exactly the same output value.

Figure 27 shows the output graph for the sway angle of the 2D Crane. Based on the figure, we conclude that the sway oscillation produced by the previous methods is the same as using the state-space approach. The detail analysis for the behavior of the 2D Crane are taken from the differential equation method as we concluded that the output graph will be in the same range.

4.13 Simulation of PID Controller of 2D Crane System

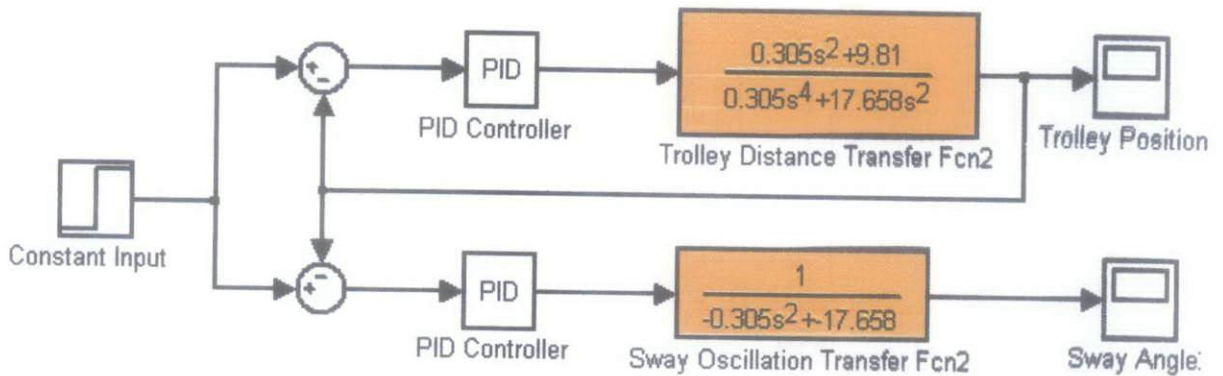


Figure 28: PID Controller of 2D Crane

Based on Figure 28, the bang-bang input force is replaced with the constant input force. This is important in order to avoid the trolley to turn back around to its original position. In simulation of this 2D Crane System, the disturbance force such as impulse force is neglected. First of all, the simulation of 2D Crane Controller system will be tested with constant input force and self-tuning values of PID constants in order to make sure the modification is functioning well for the system.

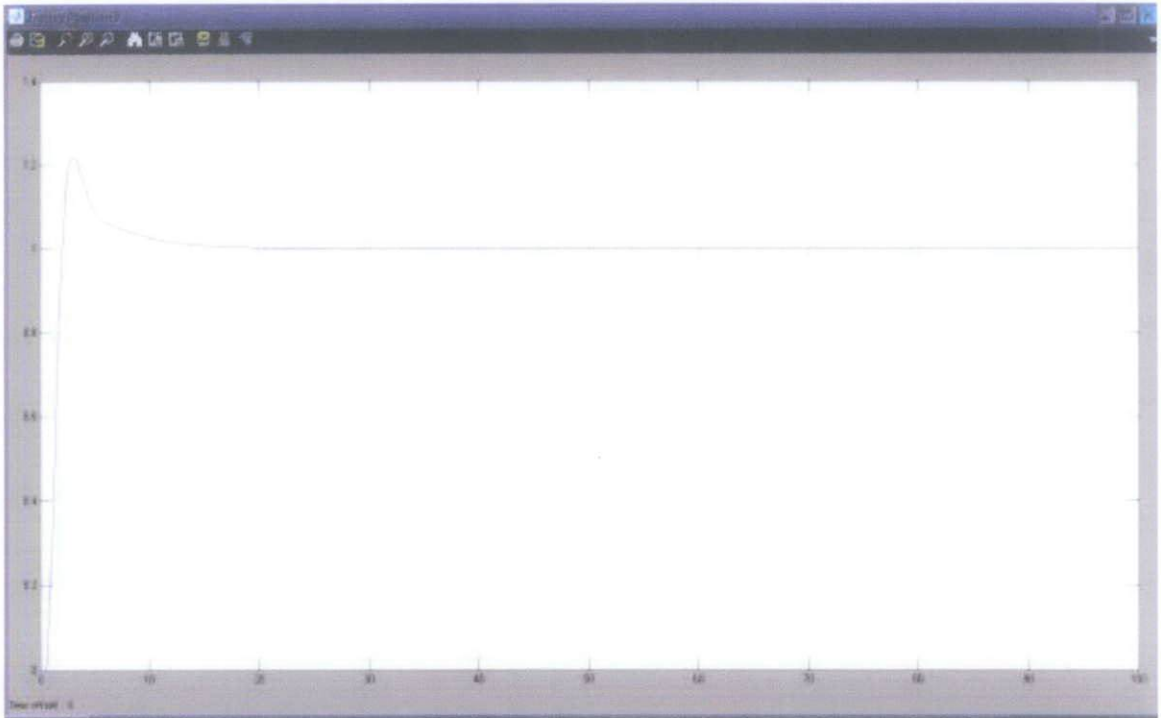


Figure 30: Trolley Position output for PID Controller of 2D Crane System

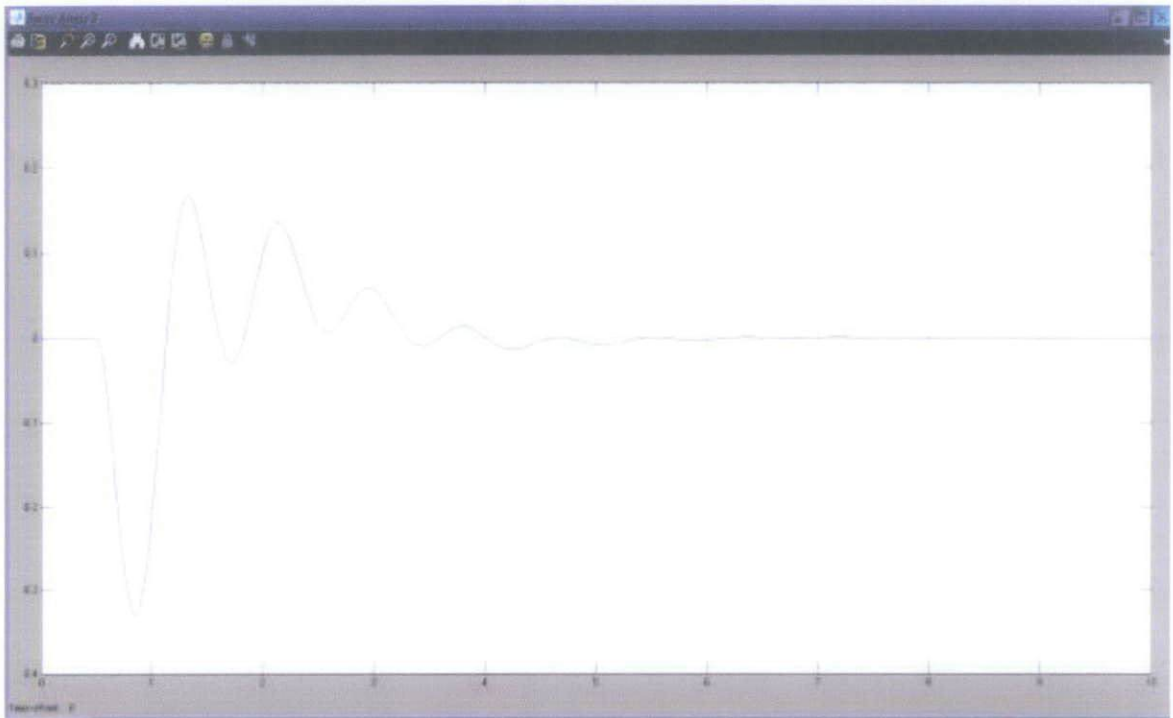


Figure 31: Sway Angle output for PID Controller of 2D Crane System

Based on the Figure 30, the trolley travelled 1m after 1N of constant input force is applied and also results in the stable payload oscillation after 3.5s thus results in a better 2D Crane System compare to the conventional system used without PID Controller.

4.13.1 Time Delay

The next figures are results of adding 5ms time delay into the output of the trolley distance travelled transfer function or state-space. The results of the output are delay for 5ms in order to obtain more accurate and reliable PID Controller values.

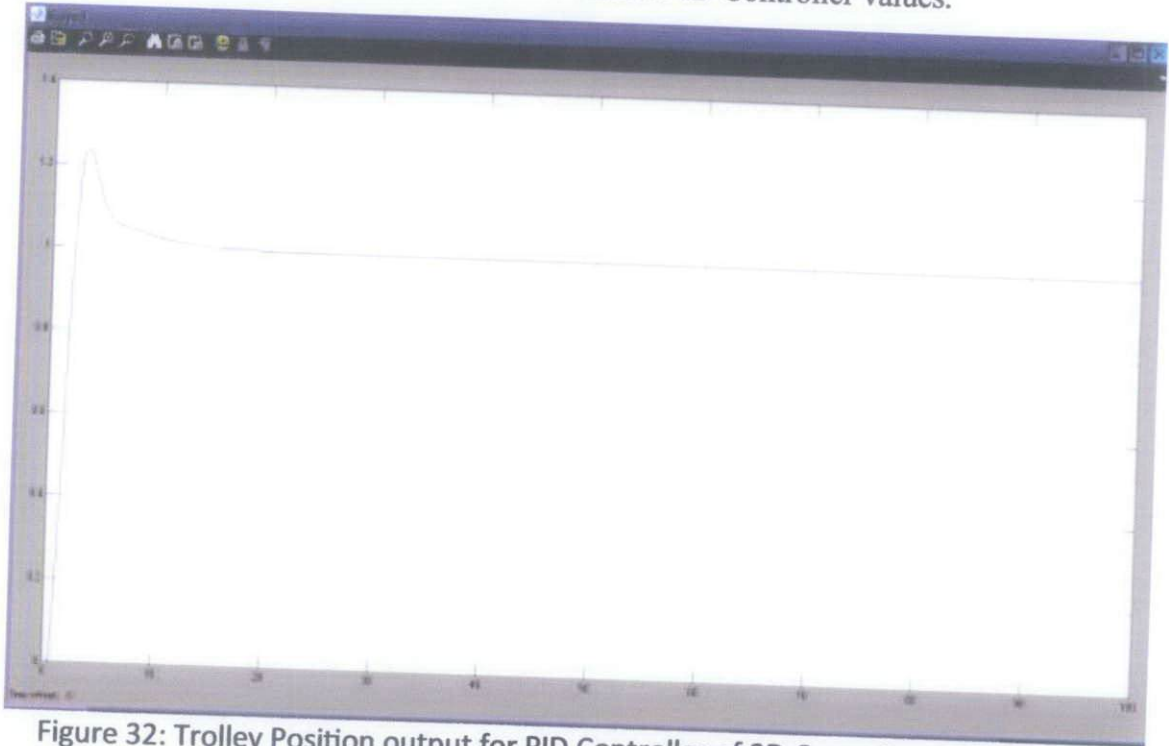


Figure 32: Trolley Position output for PID Controller of 2D Crane System with Delay

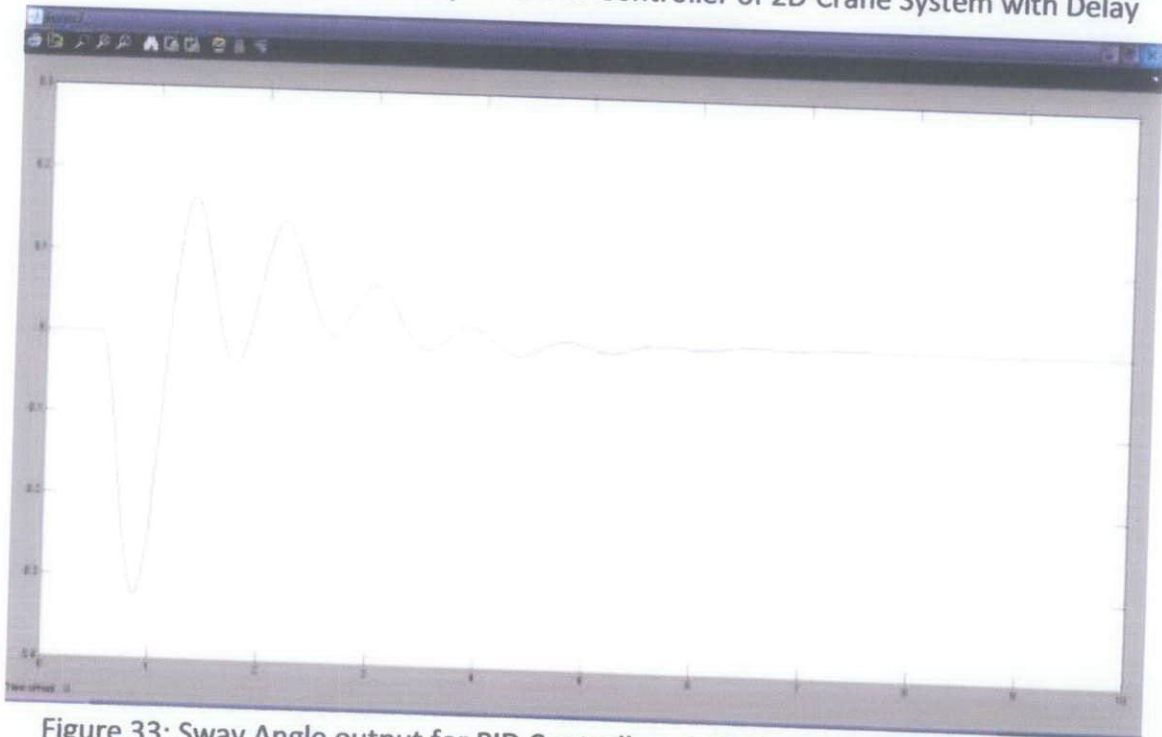


Figure 33: Sway Angle output for PID Controller of 2D Crane System with Delay

Based on the figures below, both outputs are stabilize at a constant value thus the value of PID constants used are reliable for the system.

4.13.2 Frictional Force Disturbance

The next figures are results of adding constant 0.1N frictional force as a disturbance into the output of the 2D Crane System. The distance travelled overshoot for the trolley is recorded to be 0.1N less than output results without frictional force. This is because the 0.1N fore from the constant input force are compensated by the disturbance force added into the system.

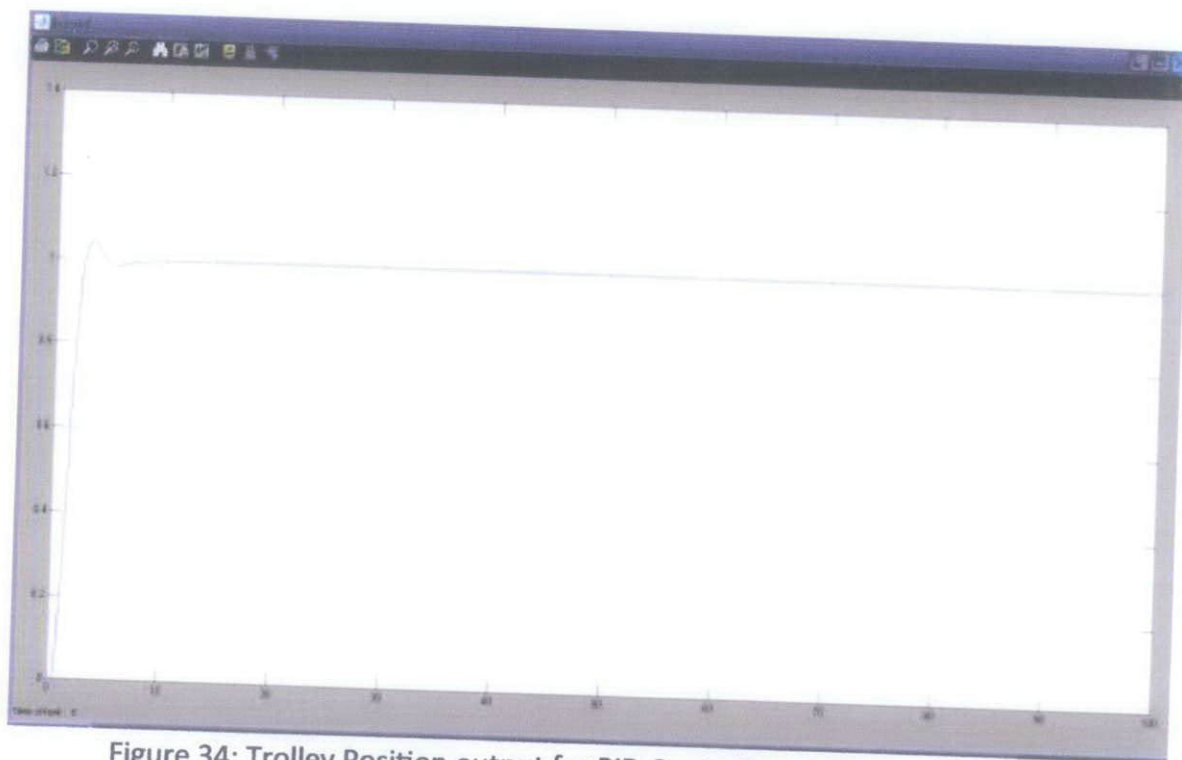


Figure 34: Trolley Position output for PID Controller of 2D Crane System with Frictional Force Disturbance and Delay

Figure 35 shows the sway angle output produced for PID Controller of 2D Crane with frictional force. The payload sway oscillation frequency is the same as the previous results without disturbance force. The payload oscillation is able to be stabilized less than 6 seconds thus improve the previous system without PID Controller which results in long period of payload oscillation and less distance travelled by the trolley.

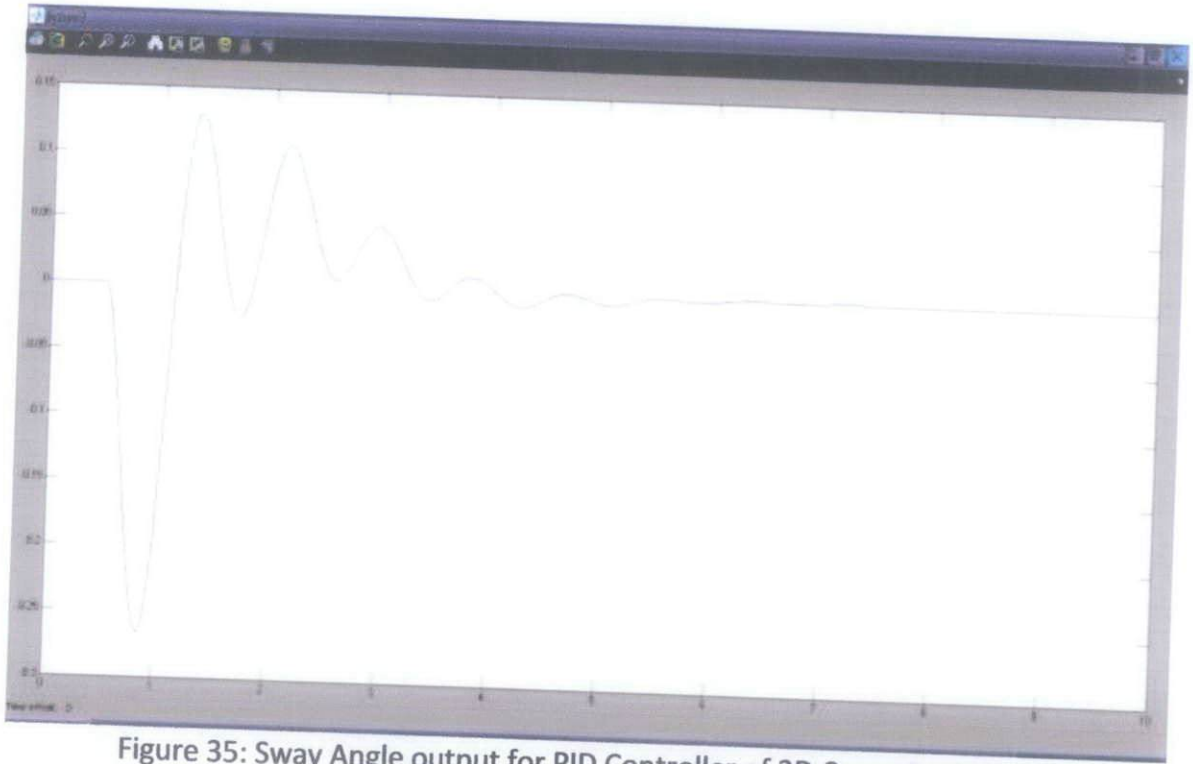


Figure 35: Sway Angle output for PID Controller of 2D Crane System with Frictional Force Disturbance and Delay

4.13.3 Harmonic Force Disturbance

The next figures are results of adding harmonic force as a disturbance into the output of the 2D Crane System. $y(t) = 1 \sin 5t$

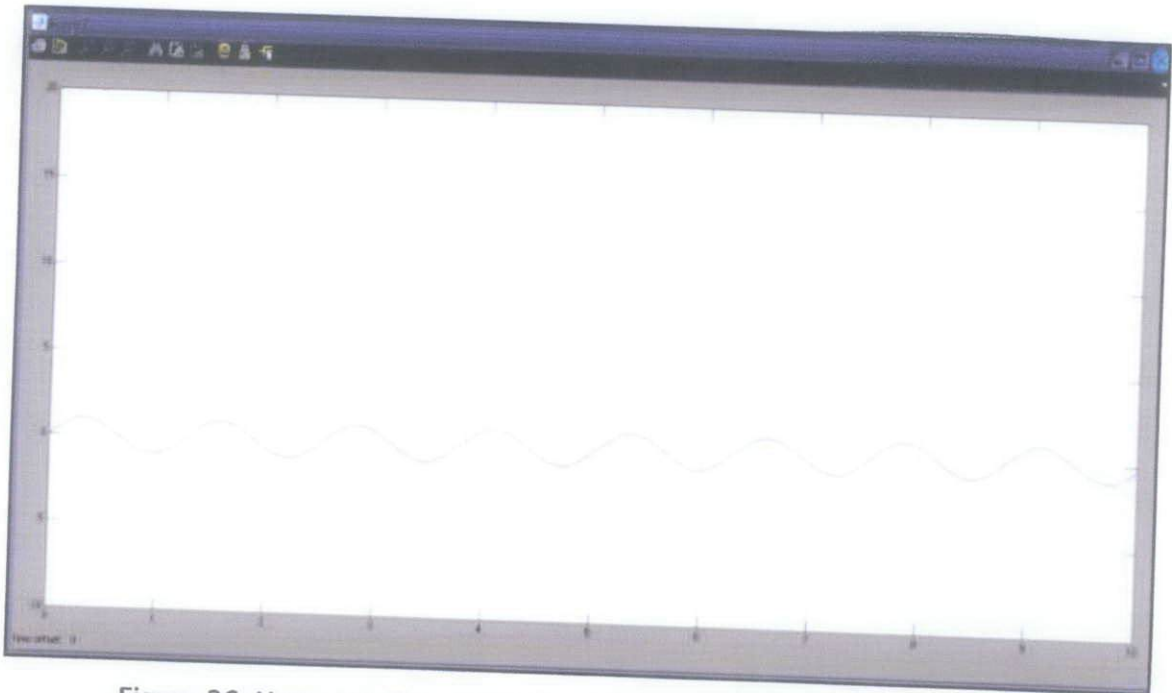


Figure 36: Harmonic Force into the 2D Crane System; $y(t) = 1 \sin 5t$

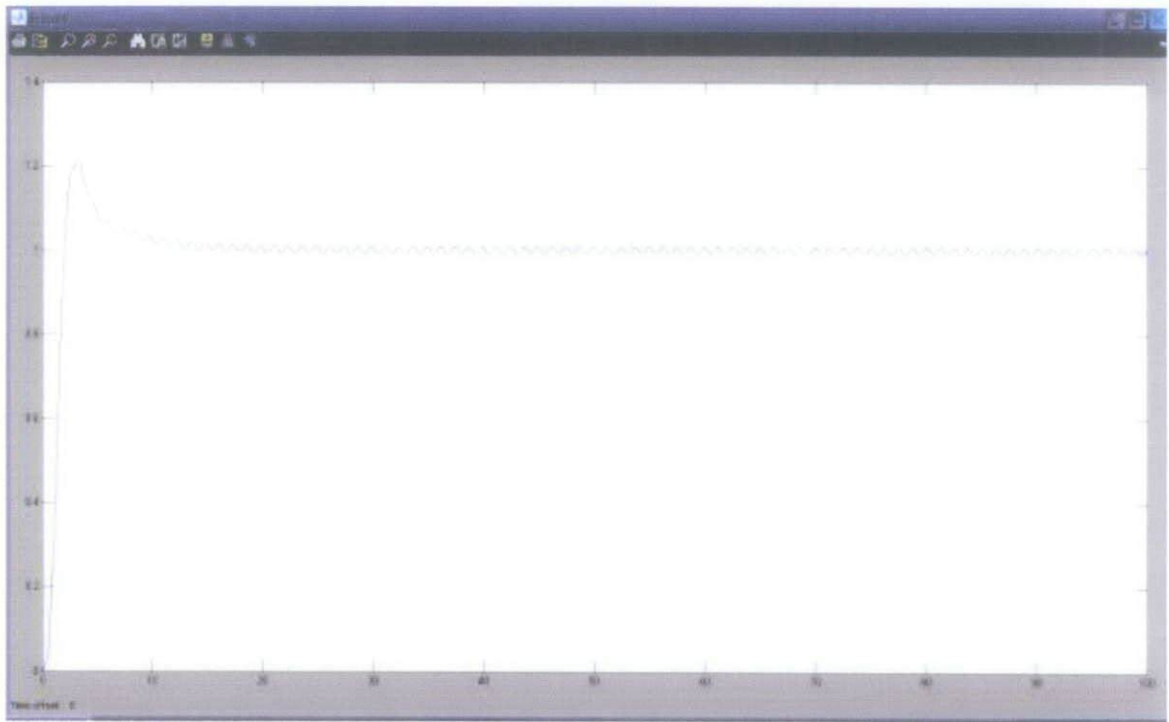


Figure 37: Trolley Position output for PID Controller of 2D Crane System with Harmonic Force Disturbance and Delay



Figure 38: Sway Angle output for PID Controller of 2D Crane System with Harmonic Force Disturbance and Delay

Based on the figures above, the trolley position is able to stabilize at constant value and sway angle output produced a constant frequency of oscillation. These may be caused by the continuous harmonic force added into the system as disturbance.

4.14 Simulation of PID Controller with Derivative Filter of 2D Crane System

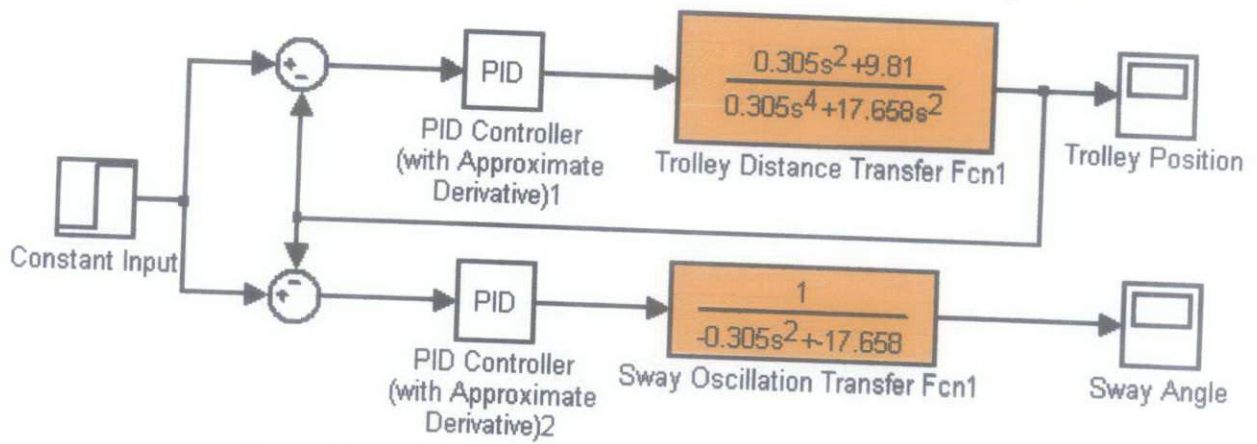


Figure 39: PID Controller with Derivative Filter of 2D Crane

Based on the Figure 39, the PID Controller with Derivative Filter is applied to the 2D Crane System in order to compare the output results with the PID Controller without Derivative Filter. In this section, the linear parameters of 2D Crane variables and PID constants are applied to the system.

In simulation using Matlab/Simulink Software for the project, below parameters are used for the PID Controller and 2D Crane state-space equation:-

- Trolley mass, $M = 1$ kg
- Payload mass, $m = 0.8$ kg
- Length of hoisting rope, $l = 0.305$ m
- Gravity, $g = 9.81$ m/s²
- Constant Input force, $F = 1$ N

PID Constant values:-

- Proportional Constant, $K_p = 5$
- Integral Constant, $K_i = 1$
- Derivative Constant, $K_d = 4$
- Derivative Divisor, $D = 100$

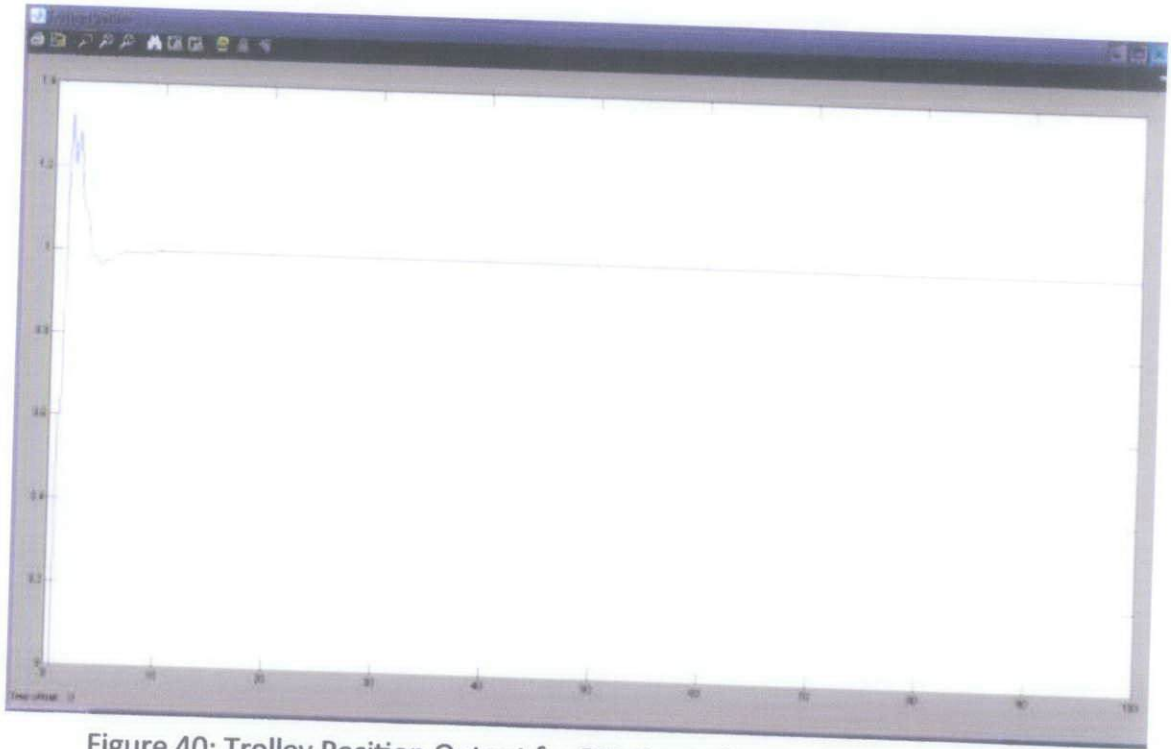


Figure 40: Trolley Position Output for PID Controller with Derivative Filter of 2D Crane System



Figure 41: Sway Angle Output for PID Controller with Derivative Filter of 2D Crane System

Based on the figures above, the results of the simulation for PID Controller with Derivative Filter of 2D Crane System is the same as the previous methods which is PID Controller without Derivative Filter.

4.15 Simulation of 3D Crane System using Differential Equation Approach

The simulation of 3D Crane System is conducted by using the differential equation approach. The general state-space equation for 3D Crane System is derived as shown below. The input for both x-direction and y-direction is separated accordingly. For y-direction, the mass of the trolley is change to mass of the trolley + mass of the metal crane

Equations can be arranged into the matrix form as below:

$$\begin{bmatrix} \dot{x} \\ \dot{\theta} \\ \ddot{x} \\ \ddot{\theta} \\ \ddot{x} \\ \ddot{\theta} \end{bmatrix} = \begin{bmatrix} 0 & 0 & 1 & 0 & 0 & 0 & 0 & 0 \\ 0 & 0 & 0 & 1 & 0 & 0 & 0 & 0 \\ 0 & \frac{mg}{M} & 0 & 0 & 0 & 0 & 0 & 0 \\ 0 & -\frac{(M+m)}{Ml} & 0 & 0 & 0 & 0 & 0 & 0 \\ 0 & 0 & 0 & 0 & 0 & 0 & 1 & 0 \\ 0 & 0 & 0 & 0 & 0 & 0 & 0 & 1 \\ 0 & 0 & 0 & 0 & 0 & \frac{mg}{M+m_c} & 0 & 0 \\ 0 & 0 & 0 & 0 & 0 & -\frac{(M+m_c+m)}{(M+m_c)l} & 0 & 0 \end{bmatrix} \begin{bmatrix} x \\ \theta \\ \dot{x} \\ \dot{\theta} \\ \ddot{x} \\ \ddot{\theta} \end{bmatrix} + \begin{bmatrix} 0 & 0 \\ 0 & 0 \\ \frac{1}{M} & 0 \\ -\frac{1}{Ml} & 0 \\ 0 & 0 \\ 0 & 0 \\ 0 & \frac{1}{M+m_c} \\ 0 & -\frac{1}{(M+m_c)l} \end{bmatrix} \begin{bmatrix} F_x \\ F_y \end{bmatrix}$$

The output equation is

$$\begin{bmatrix} x \\ \theta \end{bmatrix} = \begin{bmatrix} 1 & 0 & 0 & 0 & 0 & 0 & 0 & 0 \\ 1 & 0 & 0 & 0 & 0 & 0 & 0 & 0 \\ 0 & 0 & 0 & 0 & 1 & 0 & 0 & 0 \\ 0 & 0 & 0 & 0 & 1 & 0 & 0 & 0 \end{bmatrix} \begin{bmatrix} x \\ \theta \\ \dot{x} \\ \dot{\theta} \\ \ddot{x} \\ \ddot{\theta} \end{bmatrix}$$

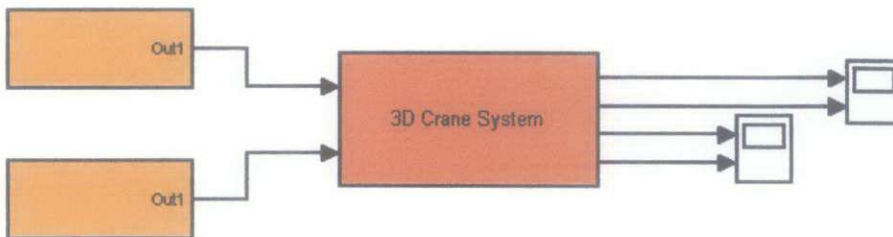


Figure 42: 3D Crane System DEE Method

Below are the values and parameters used for simulation of 3D Crane:

Trolley mass, $M = 1$ kg

Metal Crane Mass, $m_c = 2$ kg

Payload mass, $m = 0.8$ kg

Length of hoisting rope, $l = 0.305$ m

Gravity, $g = 9.81$ m/s²

Input force, $F = 1$ N

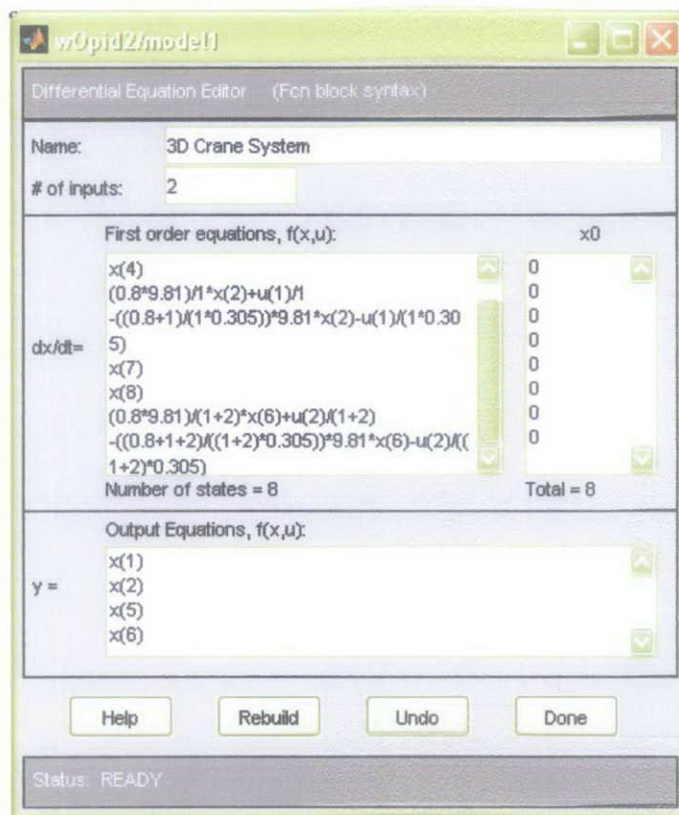


Figure 43: 3D Crane System via Differential Equation

The result for both trolley position and payload sway angle are observed as shown in Figure 44 below. The trolley position are observed to be less than the x-direction but the sway angle for 3D Crane are able to stabilize at constant point compare to the 2D Crane which results in the unstable payload sway angle. The trolley or crane travel distance for y-direction is 0.26m and maximum payload sway angle of 0.05rad.



Figure 44: Output for 3D Crane System via Differential Equation

4.16 Simulation of 3D Crane System using Transfer Function Approach

After the successful simulation of 3D Crane System via differential equation approach, the transfer function for the 3D Crane is obtained for the simulation using transfer function approach. The results of the simulation are compared to the previous method in order to verify the accuracy of the signal graph produced. Figure 45 below shows the block diagram constructed from the 3D Crane system.

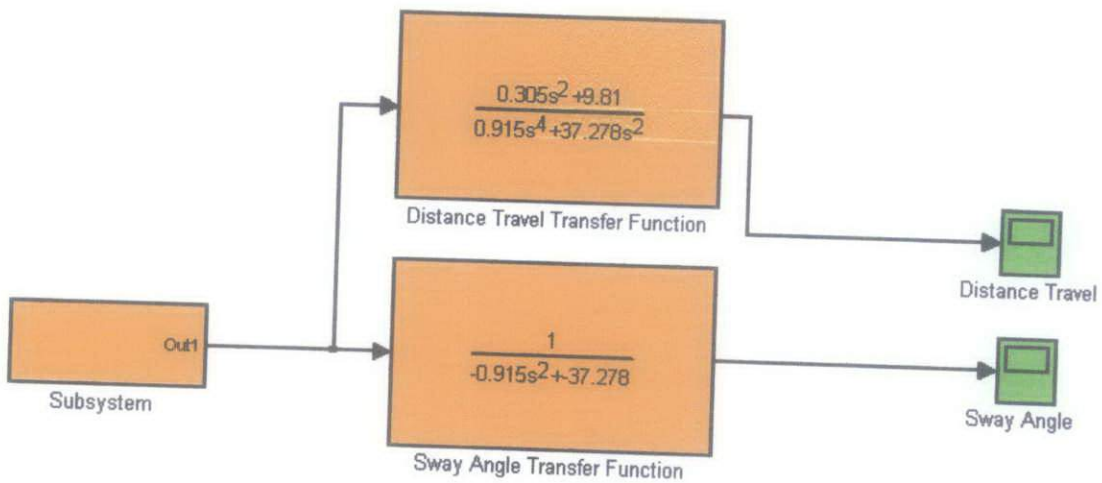


Figure 45: Transfer function obtained for 3D Crane System

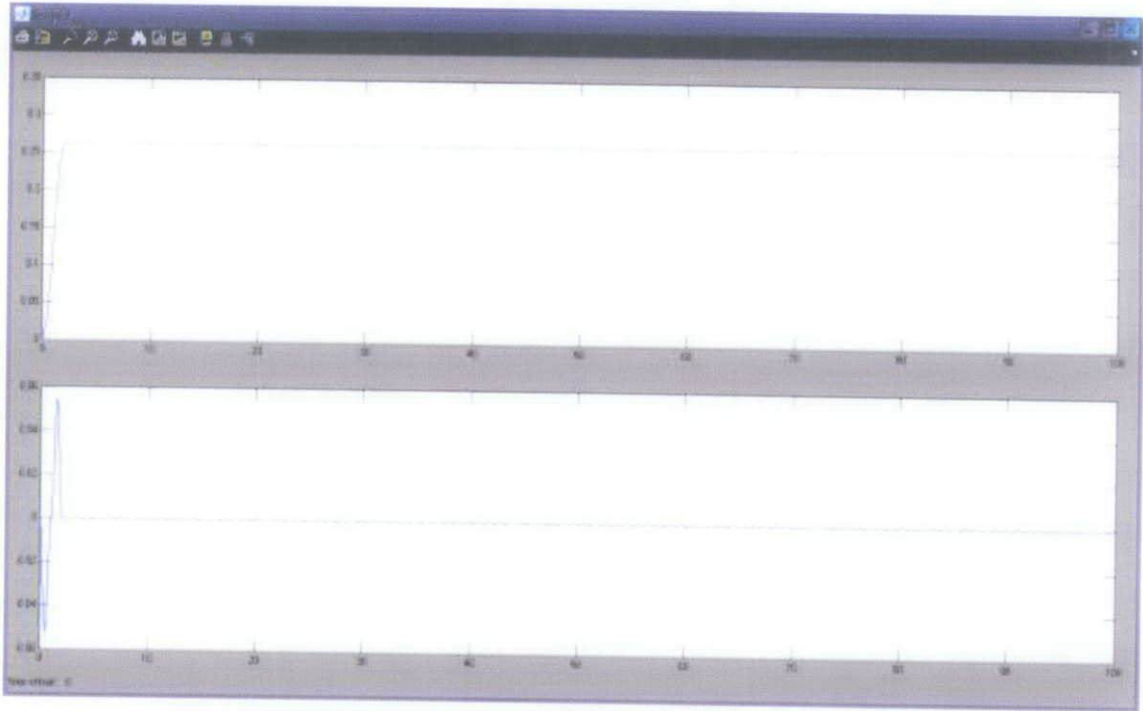


Figure 46: Output for 3D Crane System via Transfer Function

Based on the Figure 46, the output results for 3D Crane System via Transfer Function is the same as the differential equation approach, thus we conclude that the transfer function constructed for the y-direction are correct and the information obtained are enough for the next simulation and derivation of the state space equation of 3D Crane System.

4.17 Simulation of 3D Crane System via State-space Approach

After the successful simulation of 3D Crane System via transfer function approach, the state-space equation for the 3D Crane is obtained for the simulation using state-space approach. The results of the simulation are compared to the previous method in order to verify the accuracy of the signal graph produced. Figure 47 below shows the block diagram constructed from the 3D Crane system.

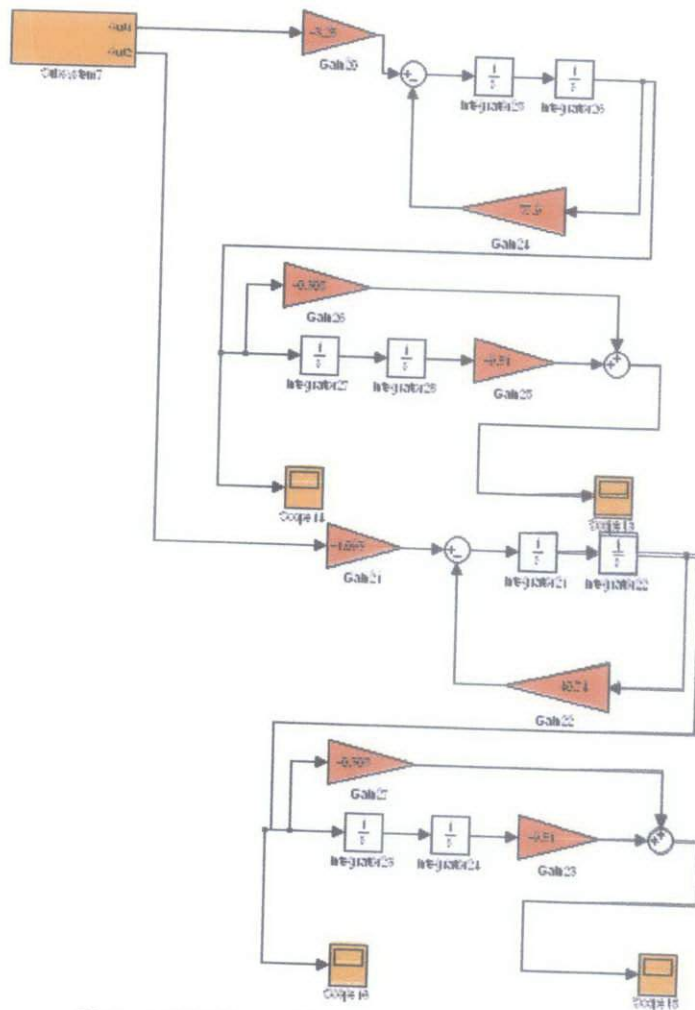


Figure 47: Crane System via State-space Approach

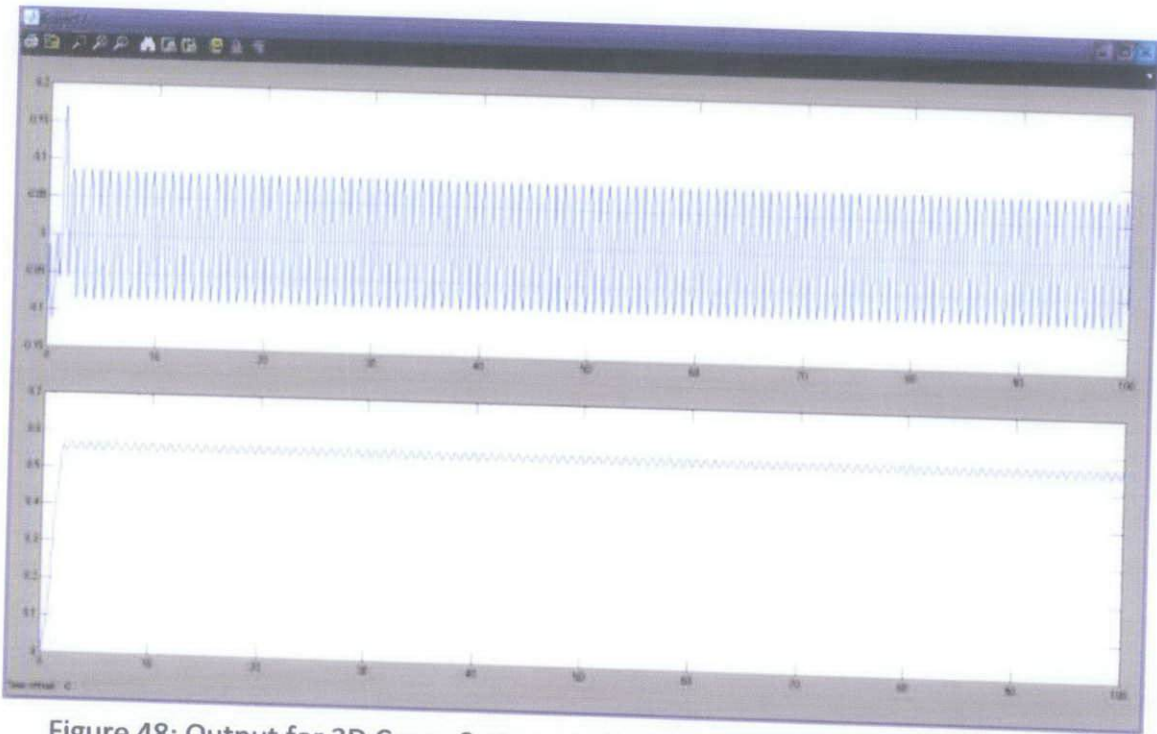


Figure 48: Output for 3D Crane System via State-space Approach for X-direction



Figure 49: Output for 3D Crane System via State-space Approach for Y-direction

4.18 Simulation of 3D Crane System Controller via State-space Approach

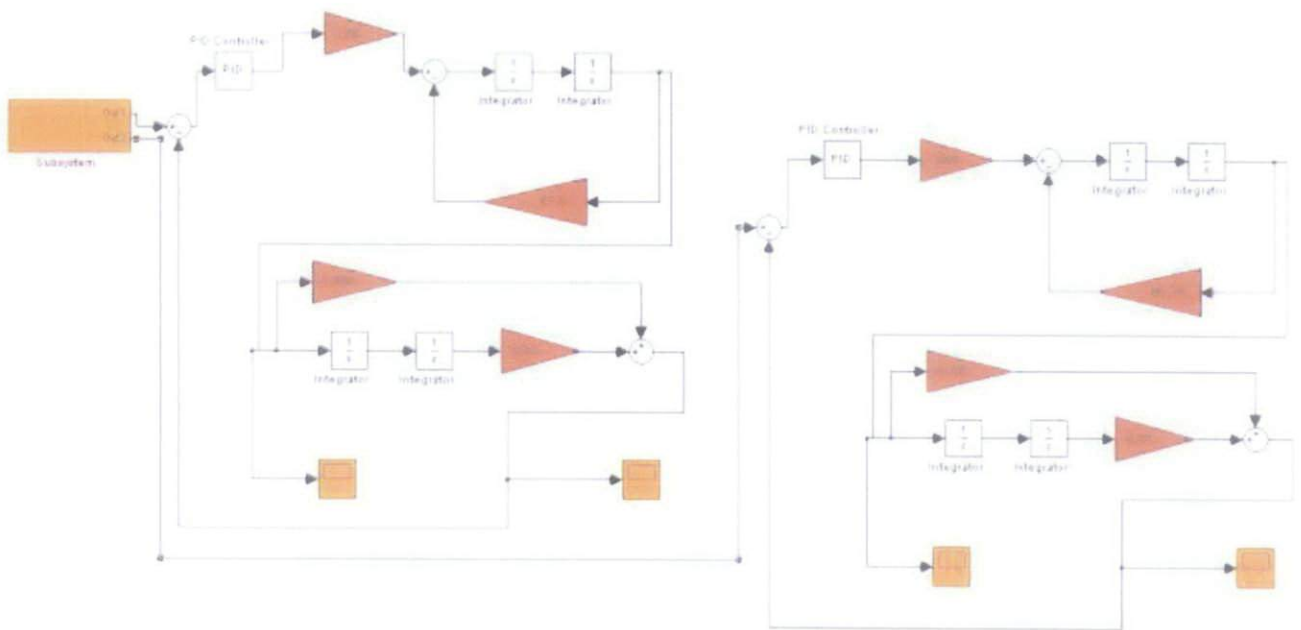


Figure 50: 3D Crane System Controller via State-space Approach



Figure 51: Sway angle for 3D Crane System with Controller via State-space Approach For x-direction



Figure 52: Trolley position for 3D Crane System with Controller via State-space Approach For x-direction

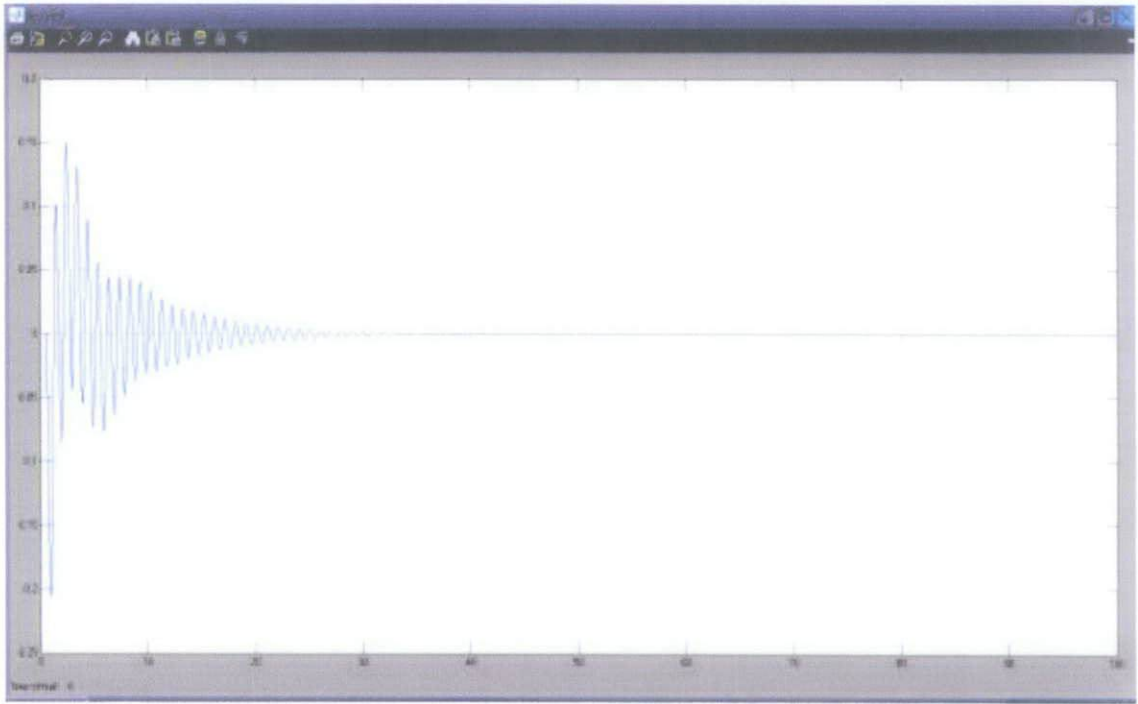


Figure 53: Sway angle for 3D Crane System with Controller via State-space Approach For y-direction

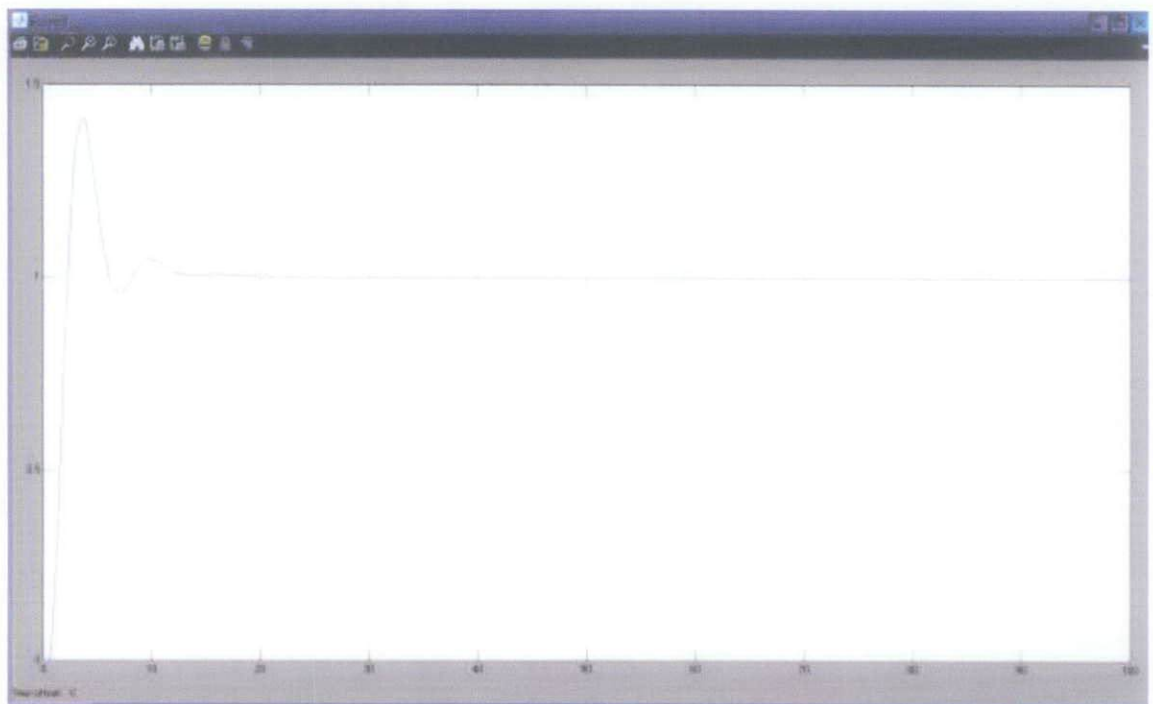


Figure 54: Sway angle for 3D Crane System with Controller via State-space Approach For y-direction

Based on the figure 51-54, by using the PID Controller, we can obtained a stabilize system with constant trolley distance for both x and y direction. For the 3D

System with PID Controller, the simulation are conducted by using the step input instead of bang-bang input force that are used for 3D Crane System without the PID Controller.

CHAPTER 5

DISCUSSION

5.0 Project Reliability

The State-space construction of 3D crane is apparently a new project in the field of Instrumentation and Control System. This project will optimized the author's understanding on the Proportional-Integral-Derivative, PID Controller and 3D crane system since the failure of crane in the process and oil and gas industries are critical as it needs to be optimized to avoid failure and decrease the plant reliability which will definitely affect the profit and decrease the plant productivity.

This project will also highlight on the automated control of a 3D crane in the plant industries thus will require author to study and conduct a detail research on understanding the automated control system use in the plant. This will definitely help author to optimize an understanding involving Instrumentation and Control System. In Instrumentation and Control System, the author has been introduced to the function of Distributed Control System, DCS and Programmable Logic Controller, PLC thus enabled author to emphasize the application of the Proportional Integral Derivative, PID Controller of the 3D Crane in detail manner.

5.1 Future Development and Application

The development of transfer function and state space equation of this 3D Crane will enable future development of 3D Crane system. Using the Simulink and Matlab, the

dynamics of the 3D Crane will be define for the future decoded into C++ and Matlab command which will enable the application of hardware connected into the system. For development of controller, the same application will be transferred into the system to optimize the applicability and reliability of the 3D Crane system. The basic linear 3D Crane can be constructed thus applying the PID Controller as define for optimization and increase plant reliability.

CHAPTER 6

CONCLUSION AND RECOMMENDATION

6.0 Conclusion

The modeling of the 3D Crane state space equation is still under process. The reliability of the equation is hopefully to be able to increase in reliability by considering the friction forces of the rail and other reliable information. After the state space equation of the 3D Crane has been successfully accomplished, the simulation of the 3D Crane system will take place. This part will consume time since it is to consider the probability of failure of the system while on construction.

Since the author is majoring in Instrumentation and Control System, this is an acceptable project to be accomplished for the fulfillment of Final Year Project since the author has the credibility as an Electrical and Electronics Engineering student and finally will enable author to have better understanding of Automation Control System.

REFERENCES

- [1] Rahman, Nayfeh, Masoud, “Dynamic and Control of Crane: a Review, Journal of Vibration and Control” 9(7), 863-908, 2003

- [2] Daqaq M.F. and Masoud, Z.N., “Nonlinear Input-Shaping Controller for Quay-Side Container Cranes, Journal of Nonlinear Dynamics”, 45, 149–170, 2006

- [3] Wikipedia, en.wikipedia.org, PID Controller

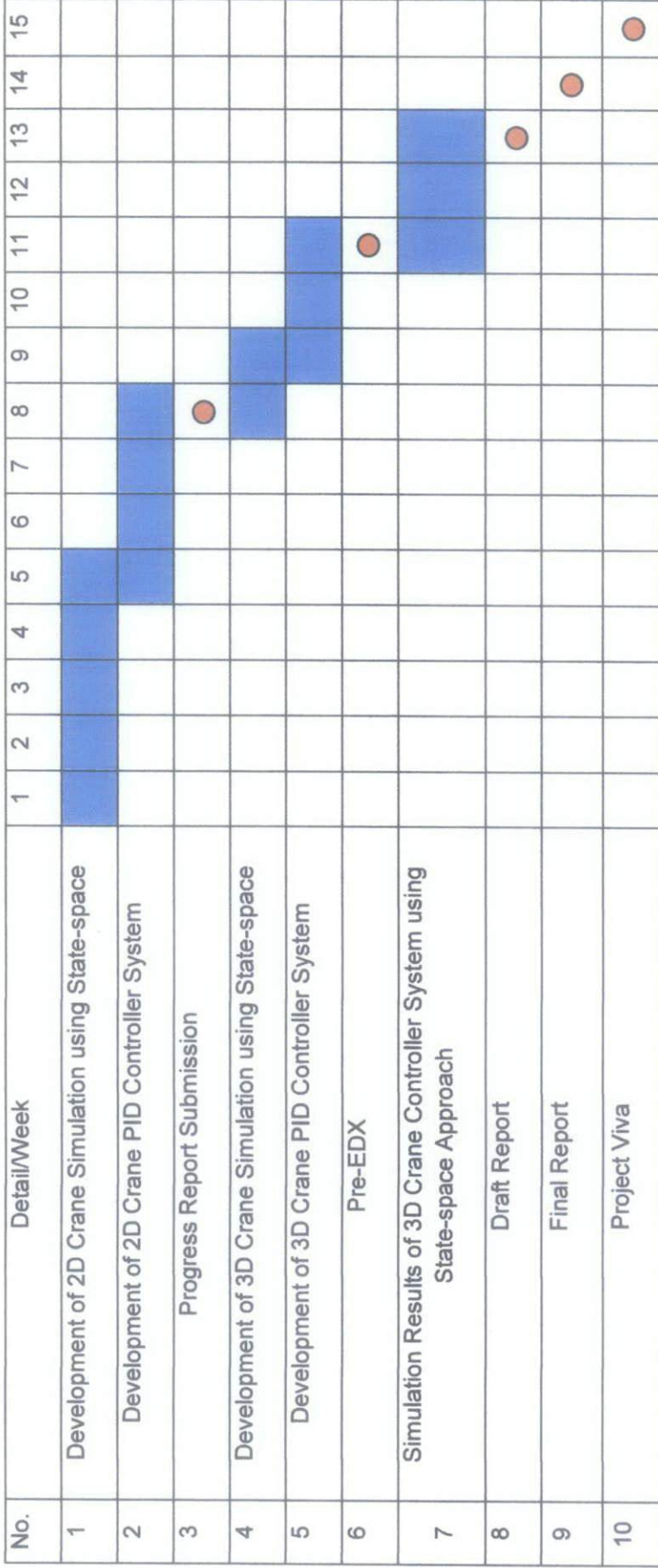
- [4] Sanda Dale, Gianina Gabor, Cornelia Gyrodi, Doina Zmaranda “Interpolative Control Algorithm Applied on a 3D-Mechatronic System”, Automation and Control System Department and Computer Science Department, University of Oradea, Romania

- [5] Thomas E. Marlin, “Process Control: Designing Processes and Control Systems for Dynamic Performance”, 2nd Edition McGraw Hill International Edition, Chemical Engineering Series, 1995

- [6] A. J. Isaksson and G. F. Graebe, “PID Control: Derivative Filter is an Integral Part of PID Design”, IEEE Explore.

APPENDIX A

Gantt chart for Final Year Project 2



REFERENCES

- [1] Rahman, Nayfeh, Masoud, "Dynamic and Control of Crane: a Review, Journal of Vibration and Control" 9(7), 863-908, 2003

- [2] Daqaq M.F. and Masoud, Z.N., "Nonlinear Input-Shaping Controller for Quay-Side Container Cranes, Journal of Nonlinear Dynamics", 45, 149–170, 2006

- [3] Wikipedia, en.wikipedia.org, PID Controller

- [4] Sanda Dale, Gianina Gabor, Cornelia Gyorodi, Doina Zmaranda "Interpolative Control Algorithm Applied on a 3D-Mechatronic System", Automation and Control System Department and Computer Science Department, University of Oradea, Romania

- [5] Thomas E. Marlin, "Process Control: Designing Processes and Control Systems for Dynamic Performance", 2nd Edition McGraw Hill International Edition, Chemical Engineering Series, 1995

- [6] A. J. Isaksson and G. F. Graebe, "PID Control: Derivative Filter is an Integral Part of PID Design", IEEE Explore.

APPENDIX A

Gantt chart for Final Year Project 2

No.	Detail/Week	1	2	3	4	5	6	7	8	9	10	11	12	13	14	15
1	Development of 2D Crane Simulation using State-space	█	█	█	█											
2	Development of 2D Crane PID Controller System					█	█	█	█							
3	Progress Report Submission								●							
4	Development of 3D Crane Simulation using State-space							█	█	█						
5	Development of 3D Crane PID Controller System									█	█	█				
6	Pre-EDX											●				
7	Simulation Results of 3D Crane Controller System using State-space Approach												█	█	█	
8	Draft Report													●		
9	Final Report														●	
10	Project Viva															●